Accepted Manuscript

Pyrimidine-chloroquinoline hybrids: Synthesis and antiplasmodial activity

Rakesh Chopra, Kelly Chibale, Kamaljit Singh

PII: S0223-5234(18)30143-0

DOI: 10.1016/j.ejmech.2018.02.021

Reference: EJMECH 10198

To appear in: *European Journal of Medicinal Chemistry*

Received Date: 16 December 2017

Revised Date: 27 January 2018

Accepted Date: 6 February 2018

Please cite this article as: R. Chopra, K. Chibale, K. Singh, Pyrimidine-chloroquinoline hybrids: Synthesis and antiplasmodial activity, *European Journal of Medicinal Chemistry* (2018), doi: 10.1016/j.ejmech.2018.02.021.

Pyrimidine-chloroquinoline hybrids: Synthesis and antiplasmodial activity

Rakesh Chopra,[♦] Kelly Chibale[♠] and Kamaljit Singh[♦,*]

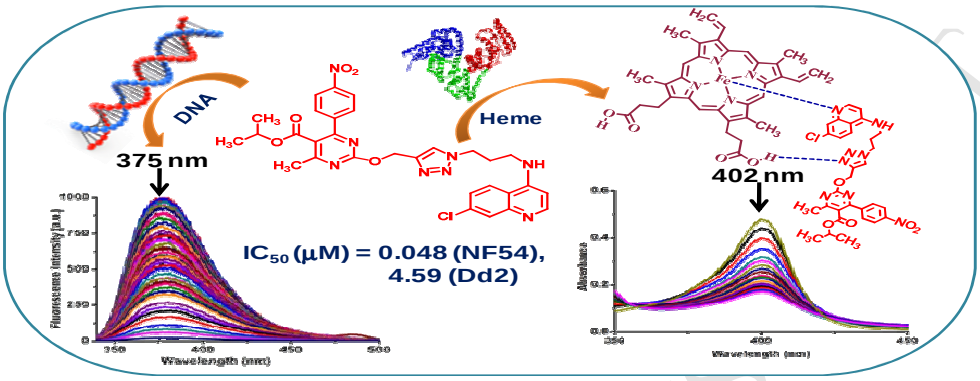

[♦]Department of Chemistry, UGC-Centre for Advanced Studies-II, Guru Nanak Dev University, Amritsar 143005, India. Email: kamaljit.chem@gndu.ac.in

[♠]Department of Chemistry, South African Medical Research Council Drug Discovery and Development Research Unit, Institute of Infectious Disease and Molecular Medicine, University of Cape Town, Rondebosch 7701, South Africa

Pyrimidine-chloroquinoline hybrids: Synthesis and antiplasmodial activity

Rakesh Chopra,[♦] Kelly Chibale[♠] and Kamaljit Singh[♦,*]

Abstract: Triazole tethered 7-chloroquinoline-pyrimidine-5-carboxylate hybrids were synthesized and evaluated for antiplasmodial activity against chloroquine sensitive (CQ^S) NF54 strain of *Plasmodium falciparum*. The most active hybrids of the series were further screened against the chloroquine resistant (CQ^R) Dd2 strain of the parasite and for *in vitro* cytotoxicity against mammalian Vero cell lines. Further, their physico-chemical properties, binding studies with hemin (monomeric & μ-oxo dimeric) and DNA [pUC-18, calf thymus (CT)] led us to plausible proposed binding mode of the most active member of the present series.

Keywords: Pyrimidine hybrids; 7-chloroquinoline; triazole; Huisgen 1,3-dipolar cycloaddition; antiplasmodial studies; lipophilicity; binding with DNA.

1. Introduction

Malaria continues to be a lead killer disease. As an estimate, a total of 216 million cases of malaria were reported by World Health Organization (WHO) in the World Malaria Report 2017, recording an increase of about 5 million cases compared to 2015. Further, nearly 445,000 deaths were attributed to malaria [1]. However, these figures represented a nearly 17.5% reduction in comparison to the malaria incidences recorded in 2010 (262 million) and a 53% decline in the number of deaths (839,000) reported in that year. At least 80% of the cases and deaths (90%) occurred in sub-Saharan Africa [1]. The disease is estimated to claim life of a child every 2 minutes in

[♦]Department of Chemistry, UGC-Centre for Advanced Studies-II, Guru Nanak Dev University, Amritsar 143005, India. Email: kamaljit.chem@gndu.ac.in

[♠]Department of Chemistry, South African Medical Research Council Drug Discovery and Development Research Unit, Institute of Infectious Disease and Molecular Medicine, University of Cape Town, Rondebosch 7701, South Africa

sub-Saharan Africa [1-4]. Malaria case incidences are highest among pregnant women and children under five years of age, owing to their weak immune system.

Out of more than 100 species of *Plasmodium* that have been identified to cause malaria, only five: *P. falciparum*, *P. malariae*, *P. vivax*, *P. ovale* and *P. knowlesi* [5] are known to cause human malaria. *P. falciparum* is responsible for the most severe form of the disease [6], and contributes most significantly to morbidity and mortality numbers associated with the disease. On the other hand, although severity of the disease caused by *P. vivax* and *P. ovale* is mild owing to persistence of dormant hypnozoite forms in the liver [7-9], they are responsible for relapses. Likewise, *P. malariae* is typically linked with chronic infections and can persist in blood asymptomatically for long periods of time [10]. The zoonotic parasite *P. knowlesi* was previously known to cause malaria only in Macaque monkeys (*Macaca fascicularis*), but has now also been reported to infect humans [11-13]. Further, various species of *Anopheles* mosquitoes are responsible for human transmission of these parasites [14].

Among the front-line drugs, artemisinin combination therapy (ACT), involving a fast acting derivative of artemisinin **1** [15,16] along with a longer-acting blood schizonticide is the treatment of choice recommended by the WHO for adults, pregnant women as well as children diagnosed with uncomplicated *falciparum* malaria [1]. The latter class of blood schizonticidal drugs are intended to minimize chances of recrudescence after clearance of the initial blood parasite load [17,18]. The most commonly implicated ACT combinations are: artemether **2**, lumefantrine **3**, artesunate **4** (ASN), amodiaquine **5**, 4-mefloquine **6**, dihydroartemisinin **7**, piperaquine **8** and 4-sulfadoxine **9** and pyrimethamine **10** (Figure 1). On the other hand, primaquine **11** is the only antimalarial known to be active [1,19] against the hypnozoite stage of *Plasmodia* and also possesses activity against *P. falciparum* gametocytes and is consequently capable of preventing transmission of the parasite [20]. However, hemolysis in glucose-6-phosphate (G6PD)-deficient individuals constitutes the major drawback [21]. The development of resistance to the one-time front-line antimalarial agents such as quinine **12**, chloroquine **13** (CQ), sulfadoxine-pyrimethamine [22,23], emerging resistance to artemisinin [24,25] and non-availability of a vaccine casts a grim picture of malaria treatment. Intense efforts are currently underway to develop antimalarials, which are active against drug-resistant mutants of *Plasmodium,* and are

both, safe, effective with minimal side effects, orally active and above all possess novel mechanisms of action.

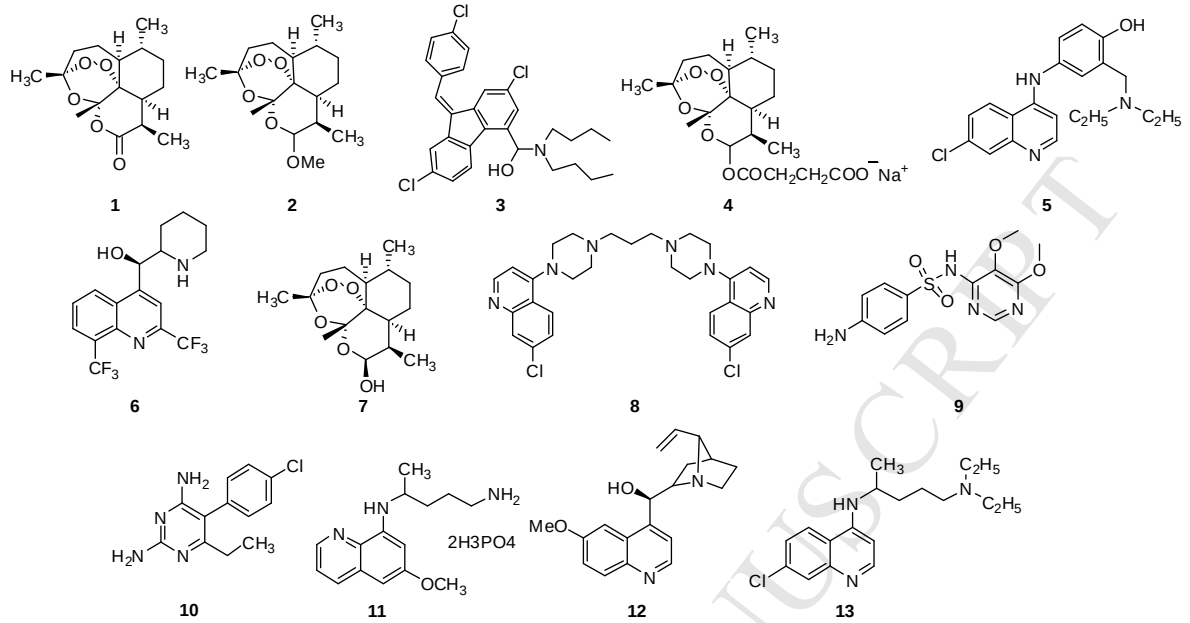

Figure 1. Chemical structures of representative ACT and chloroquine based antimalarials.

In this context, hybrid drugs are endowed with many advantages over single drug and/or multicomponent combination therapy [26-29]. These are capable of exerting dual mode of action and address issues related to drug resistance, solubility, formulation/delivery etc. In addition to structural diversity, a distinctive feature of hybrid drugs is the presence of two different antimalarial pharmacophores joined covalently, endowing them the ability to hit multiple targets. Consequently, hybrid drugs have been theme of several reviews [30-37]. Recently, synthesis and activity of a number of antimalarial hybrids based upon the pyrimidine core have been reported [38,39].

Amongst the pyrimidine hybrids, pyrimidine-4-aminoquinoline hybrids **14** containing a rigid *p*-phenylene linker exhibited moderate antipalsmodial activity [40], while the hybrids **15** (Figure 2) bearing diaminoalkane substituents on the pyrimidine core, were active in the nM range [41]. Using a 2,6-diaminopyrimidine core, Pretorius *et. al.* synthesized series of quinoline-pyrimidine hybrids **16** bearing different linkers (Figure 2), and these were active in µM range [42].

Recently, our group reported [43] pyrimidine-4-aminoquinoline hybrids **17** with potent antiplasmodial activity in the nM range. One of these hybrids **17** [R^1 = $CH(CH_3)_2$, R^2

= *o*-$NO_2C_6H_5$, R^3 = $(CH_2)_4$] proved to be the most potent of this series. Hemin and DNA binding studies indicated that these hybrids acted on multiple targets. Likewise, hybrids **18** of pyrimidine-5-carboxylates and primaquine **11** showed, both blood stage and liver stage activity against NF54 strain and *P. berghei*, respectively [43]. Further, these hybrids exhibited a higher (upto 6.7 times) liver stage activity compared to **11**. Likewise, hybrids **19-23** lacking 5-carboxylate units [44] depicted nM range *in vitro* antiplasmodial activity against the chloroquine sensitive (CQ^S) D10 and chloroquine resistant (CQ^R) Dd2 strains of *P. falciparum*. The activity was 3.2 times more than CQ [IC_{50} = 140 nM] and comparable to artesunate [IC_{50} = 31.2 nM] against the Dd2 strain.

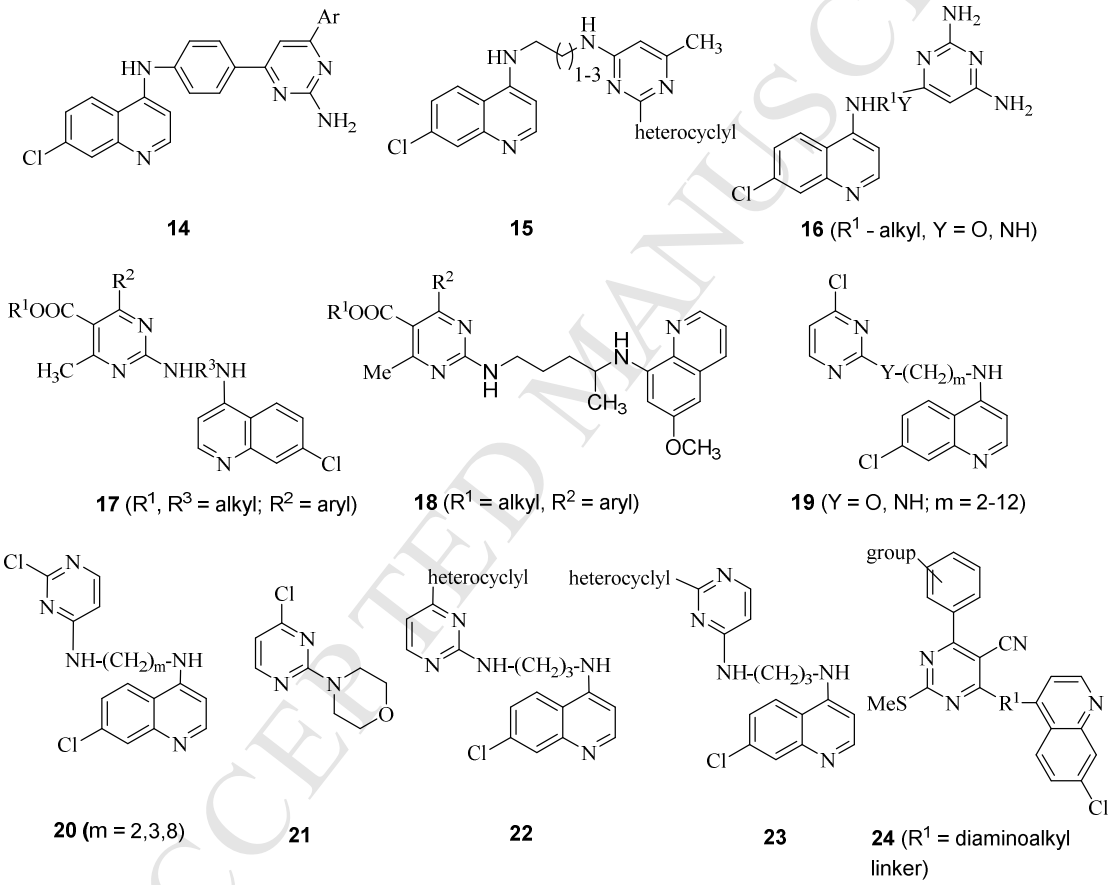

Figure 2. Pyrimidine based antimalarial hybrids.

Further, the *in vitro* antiplasmodial testing of pyrimidine-quinoline hybrids **24** (Figure 2) bearing a nitrile functionality at the C-5 position of pyrimidines [45] against two strains (NF54 and Dd2) of *P. falciparum* revealed that most of the hybrids displayed activity in nM range and seemed to inhibit hemozoin formation [45].

The quest for developing new hybrids led us to employ heterocyclic moieties such as 1,2,3-triazoles in view of their medicinal potential [46-48]. Further, 1,2,3-triazoles are stable as well as readily available through efficacious synthesis. In the present investigation, we report synthesis and antiplasmodial activity of 1,2,3-triazoles tethered 7-chloroquinoline-pyrimidine-5-carboxylates hybrids **30a-l** and **32a-f**. These were initially tested against the NF54 strain. Hybrids **30a-f** and **30h-l**, were found to be the most active hybrids in this series against the NF54 strain and were also tested against the Dd2 strain. Further, hybrids **30a-f** and **30h-l** were further screened for *in vitro* cytotoxicity against the mammalian Vero cell line. Physicochemical properties such as aqueous solubility (S_w), pK_a, log *D* were also determined. We also conducted hemin (monomeric & μ-oxo dimeric) and DNA [pUC-18, calf thymus (CT)] binding studies in order to explore the mode of action of these hybrids.

2. Results and discussion

2.1 Synthesis and characterization

Two series of 1,2,3-triazole tethered pyrimidine-chloroquinoline hybrids **30** and **32** were prepared as outlined in Scheme 1.

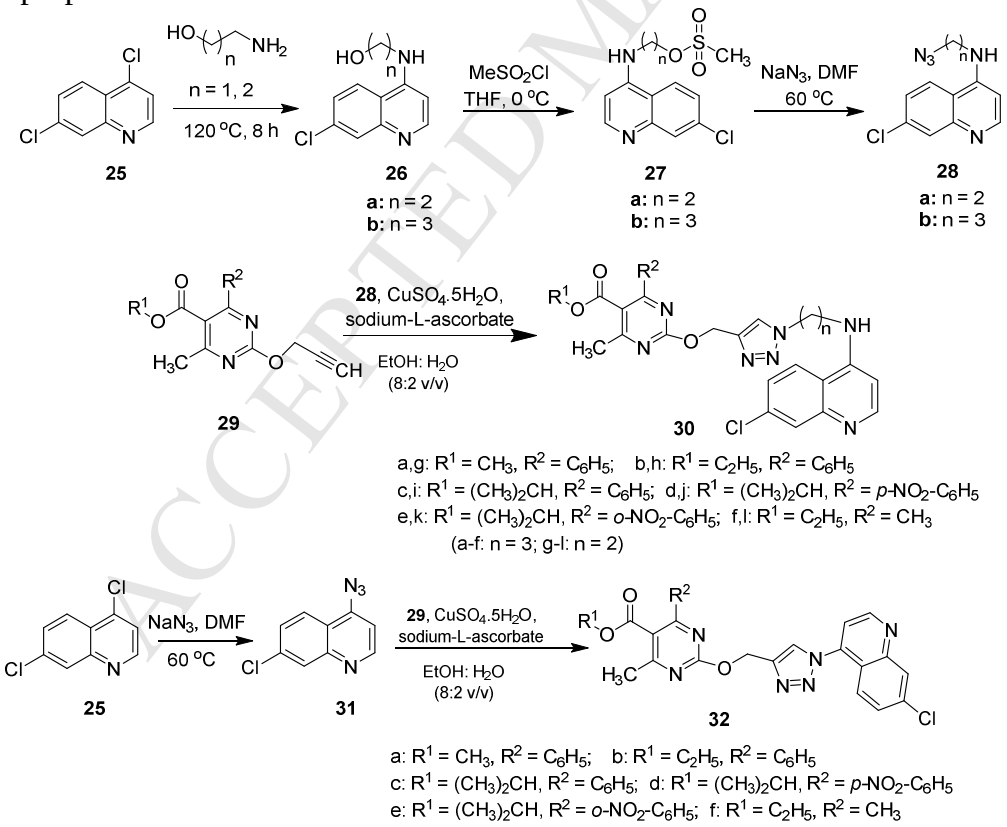

Scheme 1. Synthesis of pyrimidine-chlororoquinolinetriazole tethered hybrids **30** and pyrimidine-chloroquinolinetriazole tethered hybrids **32**.

For preparing **28** (Scheme 1), **25** was treated with the appropriate amino alcohol to give 4-hydroxyethyl/propyllamino-7-chloroquinoline **26**. Treatment of **26** with methane sulphonyl chloride in dry THF and triethylamine (Et_3N) furnished mesylated intermediate **27**, which upon treatment with sodium azide in dry DMF yielded **28**. The C-2 propargylated pyrimidines **29** were synthesized from the appropriate dihydropyrimidin-2-(1*H*)-one (obtained via conventional Biginelli condensation) [49] through pyridinium chlorochromate (PCC) mediated dehydrogenation to furnish the corresponding oxidized intermediate [50]. Subsequent treatment in refluxing $POCl_3$ furnished chloropyrimidine [51], which upon nucleophilic substitution reaction with propargyl alcohol under basic conditions yielded **29**. In the first series of hybrids comprising of **30**, the 1,2,3-triazole ring was assembled using the click reaction of appropriate azide **28** with an alkyne **29** using sodium ascorbate and copper sulphate. For the second series of hybrids, the azide **31** was obtained from 4,7-dichloroquinoline **25** and sodium azide in dimethylformamide. Click reaction of **29** with 4-azido-7-chloroquinoline **31** using standard reaction conditions (Scheme 1) afforded the second series of triazole tethered hybrids in excellent yields (Table 1). All intermediates and products were unambiguously characterized (Fig. S1-S48) using spectroscopic and microanalytical data (*vide experimental*).

2.2 *In vitro* antiplasmodial activity of triazole tethered pyrimidine chloroquinoline hybrids and structure-activity relationships (SARs)

The *in vitro* antiplasmodial activity (Table 1) of the hybrids **30** and **32** was determined against the NF54 strain using CQ and ASN as reference drugs. The compounds **30a-f** and **30h-l**, which turned out to be the most potent against NF54 were also evaluated for their *in vitro* antiplasmodial activity against the Dd2 strain. Hybrids **30a-l** (with a spacer between the triazole and chloroquinoline rings) were more potent (Table 1) than the hybrids **32a-f** with the triazole ring directly attached to chloroquinoline ring, against both NF54 and Dd2 strains. Further, on comparison of hybrids differing only in the length of the methylene spacer between the triazole and chloroquinoline rings, it is evident that the hybrid **30a** with a three carbon methylene spacer were more potent than **30g** with two carbon methylene spacer against both the *plasmodium* strains. Similarly, **30b** was more active than **30h** [52]. Hybrid **30d**, which was most active of all the hybrids against the CQ^S strain proved to be less active against the CQ^R strain, whereas, **30j** turned out to be more potent than **30d** against the CQ^R strain (Table 1).

Replacement of the methyl ester in **30a** with ethyl and isopropyl esters to form **30b** and **30c**, respectively, led to an increase in clog *P* value as well as antiplasmodial activity in that order against NF54 and Dd2 strains (Table 1).

Likewise, among the hybrids **32a-f**, lacking a spacer between triazole and chloroquinoline unit, the ethyl ester substituted **32b** was more active compared to **32a** against the CQ^S NF54 strain. However, **32c** bearing an isopropyl ester, despite being more lipophilic than **32b** (ethyl ester), was less active than **32b**. The observed variation in the activity of these hybrids could possibly arise due to the variable accumulation of hybrids in the food vacuole (FV) of appropriate strain influencing the antiplasmodial activity. Keeping all other structural features intact, introducing a polar nitro group at *ortho*-position of the C-6 phenyl substituent on the pyrimidine ring of **30c** to produce **30e** led to a decrease in the antiplasmodial activity (Table 1). Interestingly, introduction of a polar nitro group in the *para* position of C-6 phenyl group in hybrid **30c** resulted in enhancement of antiplasmodial activity of the resultant compound **30d** compared to **30c**. This is in contrast to the above (**30c** *vs.* **30e**) trend as well as our earlier findings, where the hybrid bearing C-6 *o*-NO_2 phenyl group was more active compared to its *p*-NO_2 phenyl analogue [53]. However, the observed lower activity of **30d** (Table 1) compared to **30c** against Dd2 might be attributed to factors such as mutations in CQ^R strain leading to lower accumulation of **30d** in FV of CQ^R strain. Finally, replacing the C-6 phenyl group in **30h** with a methyl group in **30l** resulted in a decrease in antiplasmodial activity of **30l** (Table 1).

2.3 Cytotoxicity

The most potent hybrids **30a-f** and **32h-l** were also screened for cytotoxicity against the mammalian Vero cell line (Table 1) using the 3-(4,5-dimethylthiazol-2-yl)-2,5-diphenyltetrazoliumbromide (MTT) assay. The IC_{50} values (Table 1) suggested that most of the hybrids were devoid of any significant cytotoxicity. Hybrid **30d**, which was the most active against the NF54 strain exhibited high selectivity index (SI = 317.50).

Table 1. Yield, antiplasmodial activity, and cytotoxicity of the 1,2,3-triazole tethered pyrimidine chloroquinoline hybrids **30a-l/32a-f**.

	R^1	R^2	Yield (%)[a]	NF54[b] IC$_{50}$ (μM)[d,e]	Dd2[c] IC$_{50}$ (μM)[d,e]	Clog*P*[f]	Cytotoxicity IC$_{50}$ (μM)[g,h]	SI[i]
30a	CH_3	C_6H_5	86	1.01±0.10	1.65±0.22	5.555	155.65±1.55	154.10
30b	C_2H_5	C_6H_5	84	0.89±0.04	1.37±0.17	6.084	152.82±0.90	171.70
30c	*i*-C_3H_7	C_6H_5	85	0.33±0.03	0.61±0.01	6.393	28.52±3.40	86.42
30d	*i*-C_3H_7	*p*-$NO_2C_6H_4$	92	0.048±0.01	4.59±0.13	6.139	15.24±0.20	317.50
30e	*i*-C_3H_7	*o*-$NO_2C_6H_4$	89	0.60±0.04	0.86±0.06	6.139	23.35±1.1	38.91
30f	C_2H_5	CH_3	87	0.70±0.05	1.11±0.14	4.485	>201± n.d	>287
30g	CH_3	C_6H_5	89	10.38±0.30	n.d[j]	5.278	n.d	n.d
30h	C_2H_5	C_6H_5	85	1.49±0.10	2.52±0.29	5.807	149.40±2.50	100.26
30i	*i*-C_3H_7	C_6H_5	88	0.64±0.10	2.00±0.26	6.116	148.52±1.0	232.06
30j	*i*-C_3H_7	*p*-$NO_2C_6H_4$	81	0.18±0.02	0.99±0.06	5.862	149.87±2.8	832.61
30k	*i*-C_3H_7	*o*-$NO_2C_6H_4$	86	0.53±0.01	1.08±0.07	5.862	145.39±4.0	274.32
30l	C_2H_5	CH_3	82	2.49±0.20	8.14±0.17	4.208	>207± n.d	>83
32a	CH_3	C_6H_5	82	15.82±0.50	n.d	5.485	n.d	n.d
32b	C_2H_5	C_6H_5	88	12.24±2.40	n.d	6.014	n.d	n.d
32c	*i*-C_3H_7	C_6H_5	83	13.99±4.10	n.d	6.323	n.d	n.d
32d	*i*-C_3H_7	*p*-$NO_2C_6H_4$	86	7.86±0.10	n.d	6.069	n.d	n.d
32e	*i*-C_3H_7	*o*-$NO_2C_6H_4$	87	16.08±0.10	n.d	6.069	n.d	n.d
32f	C_2H_5	CH_3	85	84.15±14.2	n.d	4.415	n.d	n.d
CQ[k]	-	-	-	0.018±0.002	0.275±0.02	n.d	n.d	n.d
ASN[l]	-	-	-	<5.202±ND	0.015±0.0001	n.d	n.d	n.d
EME[m]	-	-	-	n.d	n.d	n.d	0.176±0.02	n.d

[a]Isolated yield, [b]Against CQ^S NF54 strain, [c]Against CQ^R Dd2 strain, [d]activity in μM, [e]mean of three independent experiments, [f]ClogP calculated from ChemDraw Ultra 11.0 plus, [g]Cytotoxicity determined on mammalian Vero cells, [h]50% inhibitory concentration, as determined by measuring the cell viability with MTT assay, [i]Selectivity Index (SI) is calculated as IC$_{50}$ (Vero cell line)/IC$_{50}$ (NF54), [j]not determined, Standard references: [k]chloroquine, [l]artesunate, [m]emetine.

2.4 Physicochemical parameters

Aqueous solubility (S_W) and lipophilicity represent important indicators of the pharmacokinetics of a drug in a biological system. An oral drug formulation must possess critical balance of the lipophilic and hydrophilic properties so as to pass through biological membranes and barriers to eventually enter the systemic circulation [54,55]. Various physicochemical parameters such as aqueous solubility S_W, distribution coefficient (log *D*) and pK_a of the hybrids of this series were evaluated and results are summarised in Table 2. The pK_a of quinoline-based hybrids is one of the

factors that governs accumulation of the drug in the acidic FV of the parasite [56]. The solubility in *n*-octanol (S_{OC}) was calculated from the experimentally determined S_W and log *D* data using the equation: log S_{OC} = log *D* + log S_W [57]. The aqueous solubility (S_W) in PBS (phosphate buffer saline) and log *D* in an *n*-octanol/PBS buffer mixture at the cytosolic pH 7.4 of the parasite was evaluated using HPLC (Fig. S49-S66) [58].

Table 2.[a] Acid dissociation constants (pK_a), aqueous solubility (S_w), distribution coefficient (log *D*) and solubility in *n*-octanol (S_{OC}) of **30** and **32**.

Hybrid	pK_{a1}[b]	pK_{a2}[b]	S_w (µM)	log *D*	S_{oc} (µM)[c]
30a	7.38	10.78	5.64±0.43	0.78±0.27	34.19
30b	7.49	10.90	3.11±0.89	1.19±0.01	48.3
30c	7.50	-	1.21±0.43	1.72±0.05	63.53
30d	7.15	10.65	0.55±0.14	1.43±0.02	14.87
30e	7.55	9.75	0.58±0.07	1.31±0.31	12.14
30f	7.25	-	8.01±0.09	0.42±0.17	21.24
30g	6.55	8.65	11.30±0.89	0.58±0.23	44.67
30h	7.25	10.60	3.30±0.82	0.81±0.50	21.72
30i	7.20	9.55	3.21±0.37	1.21±0.11	53.08
30j	7.40	9.15	7.03±0.25	0.88±0.28	54.38
30k	7.45	10.60	2.30±0.11	0.86±0.33	16.72
30l	7.10	10.75	19.10±0.03	0.27±0.08	35.63
32a	9.78	-	3.31±0.05	0.69±0.24	16.34
32b	9.65	-	5.47±0.87	1.08±0.37	66.22
32c	9.20	-	1.78±0.17	1.46±0.07	52.48
32d	7.70	-	4.54±0.41	1.12±0.49	60.53
32e	7.50		2.93±0.33	1.10±0.23	37.41
32f	8.30		7.18±0.89	0.39±0.12	17.78

[a]The data represents mean of three experiments conducted at 298.1 K. [b]pK_a of triazole nitrogen atom; [b]pK_a of N atom quinolone; [c]Solubility in *n*-octanol at pH 7.4, calculated from experimental aqueous solubility (S_w) and distribution coefficient log D (*n*-octanol/PBS buffer) using equation: log S_{OC} = log D + log S_w.

Reasonable correlations could be drawn between the calculated distribution coefficients (Table 2) and the observed trends in the antiplasmodial activity of the hybrids. Most of the potent hybrids **30a-f** (n = 3) group have higher clog *P* and log D values compared to the analogues **30g-l** (n = 2). The more lipophilic **30a** [log *D* =

0.78, clog *P* = 5.555, IC_{50}= 1.01 μM (NF54) and 1.65 μM (Dd2)] is also more potent than **30g** [log *D* = 0.58, clog *P* = 5.278, IC_{50}= 10.38 μM (NF54)]. Similarly, **30b** [log *D* = 1.19, clog *P* = 6.084, IC_{50} = 0.89 μM (NF54) and 1.37 μM (Dd2)] being more lipophilic is more active than **30h** [log *D* = 0.81, clog *P* = 5.807, IC_{50} = 1.49 μM (NF54) and 2.52 μM (Dd2)].

Since quinoline-based hybrids are expected to accumulate in acidic FV of the parasite in much the same way as CQ and inhibit hemazoin formation, pK_a's of the synthesized hybrids **30** and **32** were determined [59] using UV-visible absorption spectrophotometric titrations (Fig. S67-S102) and the data is summarized in Table 2. Hybrids **30** and **32** showed insignificant variation in the pK_a values. The higher magnitude of the pK_a values (Table 2) suggest significant basic character of these hybrids and are thus expected to accumulate in the FV of the parasite. However, the antiplasmodial activity of these hybrids bears no regular trend with the experimentally determined pK_a values, which was not unexpected as other factors such as lipophilicity etc. also important parameters influencing activity.

2.5 Mode of action studies

2.5.1 Interaction with hemin chloride

4-Aminoquinoline base antimalarials are known to exert their antiplasmodial effect by complexation with Fe^{3+}PPIX thus inhibiting the polymerization of toxic heme to hemozoin [60,61]. In order to rationalize the binding mode of this series of hybrids, interaction of the most potent member **30d** of the current series with hemin chloride was studied by performing spectrophotometric titrations at pH 7.4 and 5.6 (approximate pH of parasitic FV) [62]. Hemin is expected to be in monomeric state in 40% aqueous DMSO solution [56]. Coupled with this, the higher clog P (6.13) of **30d** compared to CQ (5.10) suggested the use of a mixture of aqueous buffer/DMSO as solvent. The UV-visible absorption spectrum (Figure 3) recorded a gradual decrease in the intensity of the Soret band (Fe^{3+}PPIX) at 402 nm, upon incremental addition (upto 40 μM) of **30d** in hemin chloride solution, both at pH 7.4 and 5.6. Further increase in concentration of **30d** did not lead to any significant change in absorbance of the Soret band.

As CQ is known to interact with dimeric μ-oxoheme, the interaction between μ-oxoheme and **30d** (Figure S105) was also determined at pH 5.8 [63,64]. The UV-visible absorption spectrum (Figure S105A) showed a gradual decrease in the intensity

of the Soret band (Fe^{3+}PPIX) at 360 nm, upon incremental addition of **30d** (upto 26.7 µM) to hemin chloride solution (10 µM) in 20 mM phosphate buffer saline (pH 5.8). Employing Job's method of continuous variation, a 1:1 stoichiometry of the most stable complex between **30d** and monomeric hemin chloride and μ-oxoheme was established (Figure S103 and S105B). The binding constants (log K = 5.434, Table 3) for complex of **30d** with momomeric heme and μ-oxoheme, were calculated using Hyp-Spec, a non-linear square fitting programme [65], which suggested stronger binding of **30d** with μ-oxoheme. For comparison purposes, similar titrations (at pH 7.4 and 5.6) of monomeric hemin chloride were also performed with CQ (Figure S104). The binding constants of **30d** were found to be less than standard CQ consistent with the observed trend of the antiplasmodial activity (Table 1). The decrease in pH from 7.4 to 5.6 resulted in only an insignificant change in the binding constant, which suggests strong binding of **30d** with hemin chloride at both the experimental pH values.

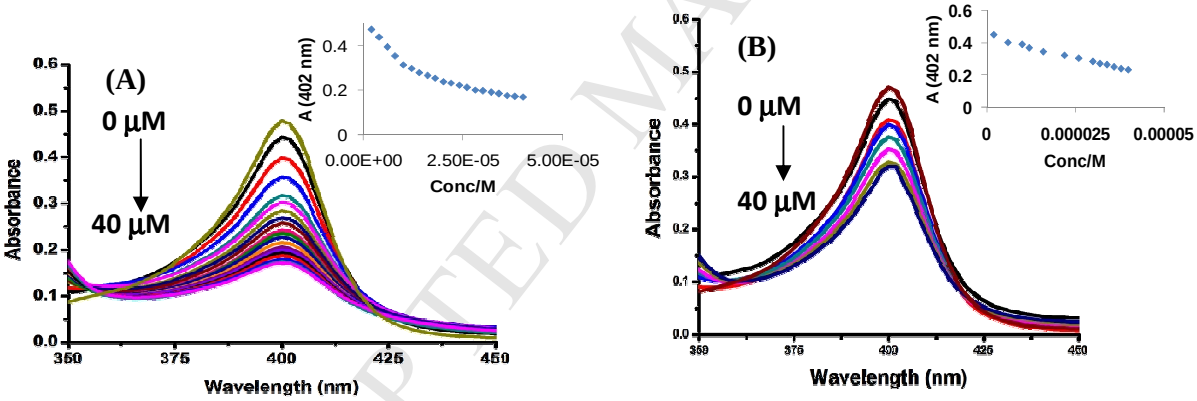

Figure 3. (A) Changes in absorption of monomeric hemin chloride (402 nm) (2.4 µM) at pH 7.4 (0.02 M HEPES buffer) and (B) at pH 5.6 (0.02 M MES buffer), upon incremental addition of **30d** (up to 40 µM). (Inset: Plot of $A_{402\ nm}$ *vs.* conc.)

Thus, we propose that hybrid **30d** and other hybrids of this series in analogy could potentially inhibit hemozoin formation by blocking the growing face of heme. Further, to provide evidence for inhibition of β-hematin formation by complexation of heme with **30d**, polymerization of hemin chloride into β-hematin was carried out at 60 °C in sodium acetate buffer (4.5 µM) [66]. FT-IR for β-hematin exhibited peaks at 1209 and 1662 cm^{-1}, characteristic of iron carboxylate bonds (Figure S106A). However, the FT-

IR of the complex prepared according to a literature report [67] upon incubation of 1.2 equiv of **30d** with hemin chloride showed absence of these peaks, which further corroborated complexation of hemin chloride with **30d** (Figure S106B). Also, the FT-IR spectrum of the complex prepared as above differ significantly from that of both **30d** (Figure S107A) as well as hemin chloride (Figure S107B).

Table 3. Binding constant (log *K*) of **30d** and CQ with hemic chloride (pH 7.4), *μ*-oxo dimeric heme (pH 5.8), CT DNA and pUC18 DNA.

	log K			
	hemin[a]	***μ*-oxo dimeric heme**	**CT DNA**	**pUC18 DNA**
30d	4.679± 0.0104 (4.274± 0.0284)	5.434 ±0.3162	3.74	3.92
CQ	5.16±0.0230(4.67±0.6546)	n.d	n.d	n.d

[a]*Values in parenthesis correspond to the titration at pH 5.6; n.d: not determined.*

To obtain further insight into the binding interaction of **30d** with monomeric hemin chloride, ^{1}H NMR titration of a solution (40% DMSO-d_6 in D_2O) of **30d** was performed with increasing concentration of hemin chloride (Figure 4). Upon addition of 10 mol% of hemin chloride, the spectra depicted significant shift (Figure 4) in the relevant signals, indicative of an interaction between hemin chloride and hybrid **30d**. Subsequent addition of hemin chloride (20 mol%) led to considerable broadening of the ^{1}H NMR peaks possibly due to increased concentration of the paramagnetic Fe^{3+}PPIX.

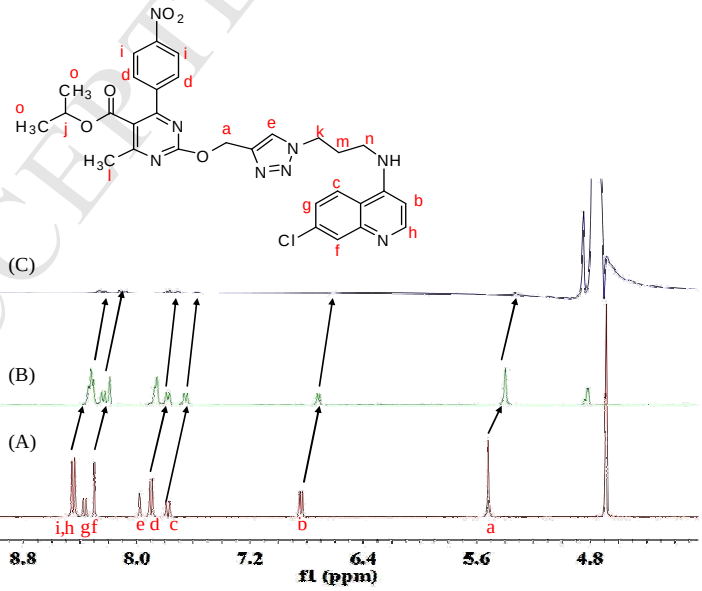

Figure 4. ^{1}H NMR spectral changes of **30d** [40% DMSO:D_2O\D_2SO_4 (10 µl)] upon incremental [0, 10 and 20 mol% (A-C, respectively)] addition of hemin chloride.

Further, HRMS mass spectrum (Figure 5A) of equimolar mixture of **30d** and hemin chloride in (40% DMSO+H_2O) exhibited a peak at *m/z* 1268.3775 corresponding to the formula $C_{64}H_{61}N_{12}Cl_2O_9Fe$, which further corroborated a 1:1 stoichiometry of the complex formed between **30d** and hemin chloride. Thus, on the basis of results obtained above as well as according to literature precedence [68], we propose an interaction between the iron atom of hemin chloride with the quinoline nitrogen as shown in Figure 5B.

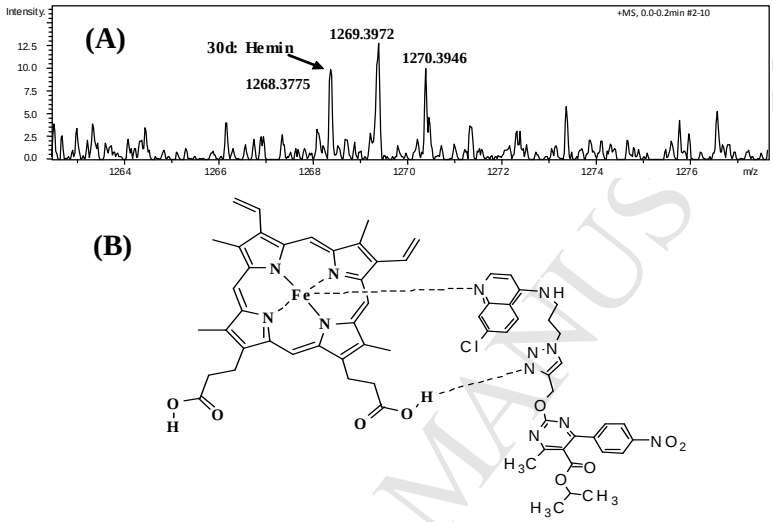

Figure 5. (A) The solution phase mass spectra of **30d** (5 µmol) upon addition of hemin chloride (5 µmol) in 40% aq. DMSO solution. (B) Proposed binding model of **30d** with hemin chloride.

2.5.2 DNA binding studies

Ionic interactions between protonated amine residues of the drugs and phosphate groups of DNA [69,70] and/or interaction between the nucleotide bases of DNA and the aromatic nucleus of a drug may result in the enhanced stability of DNA helical configuration towards thermal denaturation. The buffering action of CQ improves gene transfection efficiency by inhibiting lysosomal enzyme degradation or by facilitating the release of DNA from endocytic pathways [71]. The DNA of *P. falciparum* has poor GC content (17-19%) [72] compared to the human DNA (43%). However, CQ is known to bind predominantly to GC rich DNA. Thus a decisive relationship between antimalarial activity and DNA intercalation ability of CQ is still ambiguous. Thus, complexation studies of the most active hybrid **30d** of the current

series were undertaken with both GC rich CT DNA and AT rich pUC 18 DNA using absorption as well as fluorescence spectrophotometry.

Incremental addition of CT DNA (upto 260.42 µM) to a buffered methanolic solution (66 µM) of **30d**, showed a gradual decrease (Figure S108) in absorption at 298 nm, and characteristic quinoline bands at 330 nm. An isosbestic point was observed at 280 nm, which suggested the intercalative nature of the interaction between DNA and **30d**. The association constant (log *K* = 2.29) was calculated from the Benesi-Hildebrand equation [73]. The increase in thermal stability of DNA (Figure S109) marked by an increase in melting temperature (Table S1) of CT DNA in the presence of **30d**, further corroborated the intercalative nature of interactions [74,75].

Likewise, the incremental addition of CT DNA (upto 260.42 µM) to a solution (17.1 µM) of hybrid **30d** in buffered methanol led to a gradual decrease in emission intensity at 375 nm (Figure 6A), which eventually got completely quenched. Similar changes were observed upon incremental addition of pUC 18 DNA (upto 148 µM) to a solution (17.1 µM) of **30d** (Figure 6B). The binding constants for CT DNA (log *K* = 3.74) and pUC 18 (log *K* = 3.92) suggested that **30d** might also interact with parasitic DNA besides causing inhibition of heme polymerization to exert its antiplasmodial effect.

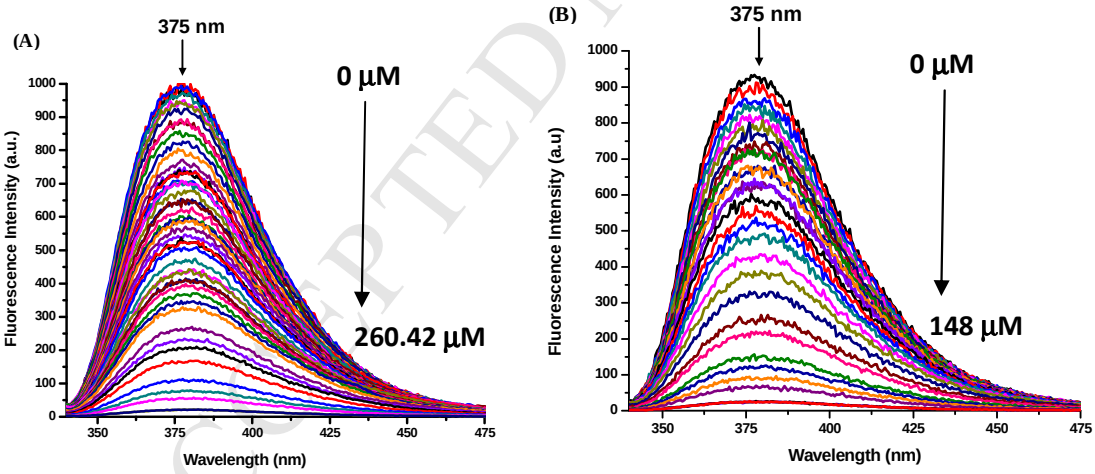

Figure 6. Changes in fluorescence emission spectra of **30d** (17.1 µM, in buffered CH_3OH, λ_{ex} = 330 nm, λ_{em} = 375 nm) upon incremental addition of (A) CT DNA (upto 260.42 µM); (B) pUC18 DNA (upto 148 µM).

3. Conclusions

A new series of 1,2,3-triazole tethered pyrimidine chloroquinoline hybrids **30a-l** and **32a-f** was initially screened for *in vitro* antiplasmodial activity against the drug

sensitive *P. falciparum* NF54 strain. The most active hybrids against NF54 were further tested against the drug resistant Dd2 strain. Hybrids **30d** and **30c** were the most potent against both strains. Cytotoxicity studies were performed against the mammalian vero cell line suggested that most of the hybrids were devoid of any significant cytotoxicity at sub-micromolar concentrations. The most potent hybrid **30d**, exhibited high selectivity index (SI = 317.50). Structure activity relationships delineated the effect of both the nature of the substituent on the pyrimidine ring and the length of the linker on the antiplasmodial activity of the hybrids. Hemin and DNA binding studies were performed for **30d** to shed light on mode of action of synthesized hybrids. The binding (DNA and hemin) studies suggest multiple site of action for these hybrids, which could also account for the observed antiplasmodial activity.

4. Experimental

4.1.1 Materials and reagents

Most reactions were performed under inert atmosphere created by using purified (oxygen free) dry nitrogen gas. Thin layer chromatography (TLC) was performed on pre-coated aluminium sheets (Merck $60F_{254}$, 0.2 mm) and the chromatograms were visualized under UV light (254 nm). For column chromatography silica gel (60–120 mesh) was employed and ethyl acetate/or mixtures of ethyl acetate/hexanes/or ethyl acetate/methanol were used as eluents. Liquid reagents used for the synthesis were purified/dried following standard drying agents and/or distilled over 4 Å molecular sieves: DCM ($CaCl_2$), CH_3CN (P_2O_5), CH_3OH/C_2H_5OH (Mg treatment), DMF (4 Å molecular sieves), tetrahydrofuran/ benzene and toluene (Na-benzophenone ketyl). K_2CO_3 was dried overnight in furnace (300°C) before use. The reagents were used as purchased. HPLC grade solvents were utilized for spectrophotometric/spectrofluorimetric studies. Recrystallization of the solid products was achieved using appropriate mixtures of DCM and hexane.

4.1.2 Instrumentation

^{1}H NMR (500 MHz) and ^{13}C NMR (125 MHz) spectra were recorded on Bruker Biospin Avance III HD (500 MHz), instrument using tetramethylsilane (TMS) as internal standard and $CDCl_3$ and/or DMSO-d_6 as deuterated solvents. The purity of the products was checked by elemental analysis performed on a Thermoelectron FLASH EA1112 CHNS analyzer and was within ± 0.4% of the calculated values. High

resolution mass spectrum (HRMS) was recorded using Bruker HRMS MICROTOF-Q II mass spectrometer. IR spectra were recorded using Perkin-Elmer FTIR-C92035 spectrometer in the range 400–4000 cm^{-1} using KBr pellets or in DCM solutions. Fluorescence measurements were performed on a Perkin Elmer LS-50 instrument. UV-visible absorption studies were carried out using UV-1800 SHIMADZU UV-Spectrophotometer using matched quartz cuvettes (path length = 1 cm). The cell holder was maintained at 25 ± 1 °C using a Peltier temperature controller. The pH titrations were performed on Equip-Tronics Digital pH meter (model–EQ 610) The HPLC chromatograms were recorded using a Waters 2489 HPLC separations module equipped with Waters 2489 photodiode array detector, Waters 515 HPLC pump with 20 μL standard sample injector, Symmetry (4.6 mm × 75 mm), 3.5 μm C-18 reverse phase column, flow rate of 0.5 mL/min., Empower software (Waters Corporation, Milford, MA, USA). A calibration plot of the peak area versus compound concentration for each compound showed excellent linearity ($0.99 < r^2 < 1$) over the concentration range (0−10 μM) employed for analysis. The purity of the products was also checked by HPLC and was ≥ 96%. All reported yields are isolated yields.

4.1.3 Determination of aqueous solubility

The aqueous solubility was determined by preparing saturated solutions in PBS (phosphate buffer saline) buffer (10 mM) at pH 7.4. The compounds were stirred in a water bath at 32 °C for 24 h. The saturated solution was filtered and the filtrate was analyzed using HPLC. Further solutions of known concentrations of test compounds were prepared in DMSO and HPLC chromatograms recorded. Plotting concentration (1×10^{-3} to 1×10^{-7} M) *vs* area under the peak furnished calibration curve. The exact concentration of the test compounds in saturated aqueous filtrate could be deduced from the calibration curve, which corresponded to the limit of solubility of the compound under the experimental conditions used.

4.1.4 Determination of partition coefficient (log *D*)

n-Octanol and PBS buffer solutions (pH 7.4) were mixed in equal volumes and were saturated with each other by stirring for 24 h and then separated. Accurately weighed **30** and **32** (0.002 g) were dissolved in 0.75 mL of pre-saturated *n*-octanol in graduated (2 mL) test tube and sonicated for 10 min. To the above sonicated solutions 0.75 mL pre-saturated PBS buffer solution was added and solutions were again sonicated for 1h

and centrifuged for 30 min at 4000 rpm. The ratio of final volume of the PBS buffer and *n*-octanol was close to 1. Aqueous and organic phases were separated and concentration of **30** and **32** in both the phases was measured by HPLC using the calibration (concentration *vs* area) curve prepared above. The log D values were calculated as logarithmic ratios of concentrations in the *n*-octanol phase compared to the concentrations in the buffer. The experiments were performed in triplicate.

4.1.5 Determination of pK_a

Stock solutions (10 mM) of compounds **30** and **32** were prepared in DMSO. The working solutions (30 µM) were obtained by diluting stock solution of a compound with distilled water so that overall DMSO content in the solution corresponded to 30% *v/v*. The pH of the solutions was adjusted to 3 by adding HCl solution (0.1 M) and in the range 3-12 using NaOH (0.1 M). The UV-visible absorption spectra were recorded in the order of increasing pH (3-12). All measurements were carried out in triplicate at 298.1 K. Plots of absorption *vs* apparent pH values at 330 nm of sample solution furnished sigmoid curves, from where pK_a values were determined as the center point in the respective titration curve.

4.2 Heme binding studies

4.2.1 Binding with monomeric heme

The stock solution (1.2 mM) of hemin chloride was prepared by dissolving hemin chloride (7.8 mg) in DMSO (10 mL). Working solution (2.4 µM) of hemin chloride was prepared by diluting (20 µL) hemin stock solution with 1 mL 0.2 M HEPES buffer (pH 7.4), 4 mL DMSO and making final volume up to 10 mL with double distilled deionized water. Likewise, the stock solution (2 mM) of **30d** was prepared in DMSO. Hemin chloride solution (2.4 µM, 3mL) was titrated with increasing concentrations (upto 40 µM) of **30d**. Subsequent to each addition of aliquot of the compound in the solution of hemic chloride, absorbance was recorded at 402 nm. Likewise, solution of hemin chloride and **30d** were titrated at pH 5.6 (2-[N-morpholino]ethanesulphonate (MES, pH 5.4) buffer was used).

4.2.2 Binding with dimeric μ-oxoheme

The stock solution (1 mM) of μ-oxoheme was prepared by dissolving hemin chloride in NaOH (0.1 M). To ensure complete dissolution of hemin chloride, solution was sonicated for 30 min. The resulting solution was subsequently diluted to achieve

working concentration (10 µM) by adding phosphate buffer (20 mM, pH 5.8). On the other hand, stock solution (2 mM) of **30d** was prepared in DMSO. Titration was performed by successive addition of aliquots of stock solution of **30d** (upto 26.7 µM) to the solution of μ-oxoheme (10 µM, 3 mL) prepared above and the absorbance was recorded at 364 nm.

4.3.1 Complexation of hemin chloride and 30d

The complex was prepared by dissolving equimolar solution of hemin chloride (15 mg) and **30d** (9.14 mg) in NaOH (0.1 N, 3mL). A solution containing 1.74 mL of aqueous sodium acetate (12.9 M, pH 5.00) and 0.3 mL of HCl (1.0 M) pre-warmed at 60 °C, was then added. After 1 h incubation at 60 °C, the reaction mixture was filtered over millipore filters (0.45 µm). The solid obtained was thoroughly washed with distilled water (3 x 30 mL) and was vacuum dried over P_2O_5. Then, the solid precipitate was characterized by FT-IR spectroscopy.

4.4 DNA binding studies

A stock solution (2 mM) of **30d** was prepared in methanol. The DNA binding experiments were carried out by diluting the stock solution of **30d** with 1:3 Tris-EDTA (10 mM Tris-HCl, 1 mM EDTA, pH 7.4) (TE) buffer/methanol. Likewise, a stock solution of DNA (pUC 18 and CT DNA) was prepared by dissolving DNA pellet in the TE buffer. The DNA concentration was estimated by comparing the absorbance intensity (260 nm) with a known molar absorption coefficient value 6600 dm^3 mol^{-1} cm^{-1}. The purity of DNA was established from ratio of absorbance intensity at 260 and 280 nm, which in the present study is 1.88, suggesting that DNA is free from protein.

The titration experiments were performed by varying the concentration of DNA and keeping the **30d** concentration constant (66.6 µM). All the UV-visible absorption spectra were recorded after equilibration of solution for 5 min. Similarly using fluorimetry, the titration was performed by varying the concentration of DNA [**30d**: CT DNA (upto 260.42 µM) and pUC 18 DNA (upto 148 µM)] and keeping the compound concentration constant (**30d**: 17.1 µM).

4.5 Thermal denaturation of DNA

DNA melting experiment was performed by monitoring the absorbance of CT DNA (151 µM NP) at 260 nm at various temperatures in absence and presence **30d**/CQ in 5:1 ratio of the DNA and **30d**/CQ with ramp rate of 0.5 °C/min in a 40% DMSO/TE

buffer (pH 7.4) with NaCl (0.5 mM). The thermal melting temperature was calculated by plotting dA/dT *vs* temperature.

4.6.1 Synthesis of alkyl 4-methyl-6-aryl-2-(prop-2-yn-1-yloxy) pyrimidine-5-carboxylates

To a solution of appropriate 2-chloropyrimidine (3.80 mmol) in dry CH_3CN (30 mL), dry K_2CO_3 (1.57 g, 11.40 mmol) and propargyl alcohol (0.32 g, 5.70 mmol) were added in that sequence and the reaction mixture was refluxed overnight. After completion (TLC), CH_3CN was removed under vacuum. Water (30 mL) was then added to the residue and the product extracted with DCM (2 x 20 mL). Dichloromethane extract was dried over anhydrous sodium sulphate and the solvent was removed under vacuum. The crude product was purified by column chromatography using ethyl acetate/hexane mixtures as eluent to obtain pure **29**. The characteristic data of compounds prepared as above is given below.

4.6.1.1 Methyl 4-methyl-6-phenyl-2-(prop-2-yn-1-yloxy)pyrimidine-5-carboxylate 29a

White solid. Yield: 94%. Rf: 0.5 (30% ethyl acetate/ hexane). Mp 69-73 °C. IR (KBr): ν_{max} 1531, 1527, 1710, 2987, 3252 cm^{-1}.^{1}H NMR (500 MHz, $CDCl_3$, 25 °C): δ 2.48 (t, *J* = 2.5 Hz, 1H, CC<u>H</u>), 2.58 (s, 3H, C-6 CH_3), 3.69 (s, C-5 O<u>CH_3</u>), 5.09 (d, *J* = 5.0, 2H, C-2 O<u>CH_2</u>), 7.43-7.50 (m, 3H, Ar<u>H</u>), 7.64-7.69 (m, 2H, Ar<u>H</u>). ^{13}C NMR (125 MHz, $CDCl_3$, 25 °C): 22.7, 52.4, 55.1, 74.9, 78.2, 120.0, 128.3, 128.4, 130.3, 137.6, 163.0, 166.2, 168.5 and 168.9. Anal. calcd. for $C_{16}H_{14}N_2O_3$: C, 68.07; H, 5.00; N, 9.92; found: C, 68.26; H, 4.85, N, 9.10. HRMS calcd. for $C_{16}H_{14}N_2O_3$: *m/z* 282.1004; found: *m/z* 282.1008 (M^+).

4.6.1.2 Ethyl 4-methyl-6-phenyl-2-(prop-2-yn-1-yloxy)pyrimidine-5-carboxylate 29b

White solid. Yield: 94%. Rf: 0.5 (30% ethyl acetate/ hexane). Mp 65-67 °C. IR (KBr): ν_{max} 1533, 1552, 1708, 2985, 3250 cm^{-1}.^{1}H NMR (500 MHz, $CDCl_3$, 25 °C): δ 1.07 (t, *J* = 5.0 Hz, 3H, C-5 OCH$_2$<u>CH_3</u>), 2.50 (t, *J* = 2.5 Hz, 1H, CC<u>H</u>), 2.61 (s, 3H, C-6 CH_3), 4.18 (q, *J* = 10.0 Hz, 2H, C-5 O<u>CH_2</u>CH_3), 5.11 (d, *J* = 2.5 Hz, C-2 O<u>CH_2</u>), 7.44-7.69 (m, 5H, Ar<u>H</u>). ^{13}C NMR (125 MHz, $CDCl_3$, 25 °C): δ 13.6, 22.7, 55.1, 61.7, 74.7, 78.2, 120.5, 128.3, 128.4, 130.2, 137.5, 163.0, 166.3, 168.1 and 168.9. Anal. calcd. for $C_{17}H_{16}N_2O_3$: C, 68.91; H, 5.44; N, 9.45; found: C, 68.95; H, 5.51, N, 9.41. HRMS calcd. for $C_{17}H_{16}N_2O_3$: *m/z* 296.1161; found: *m/z* 296.1169 (M^+).

4.6.1.3 Isopropyl 4-methyl-6-phenyl-2-(prop-2-yn-1-yloxy)pyrimidine-5-carboxylate 29c

Colourless oil. Yield: 94%. Rf: 0.5 (30% ethyl acetate/hexane). IR (dichloromethane): ν_{max} 1556, 1585, 1713, 2939, 2981, 3047, 3255 cm^{-1}.^{1}H NMR (500 MHz, $CDCl_3$, 25 °C): δ 1.09 (d, *J* = 10.0 Hz, 6H, C-5 OCH($\underline{CH_3}$)$_2$), 2.49 (t, *J* = 2.5 Hz, 1H, C$\underline{CH}$), 2.59 (s, 3H, C-6 CH_3), 5.05-5.10 (m, 1H, C-5 O$\underline{CH}$(CH_3)$_2$ and 2 H C-2 O$\underline{CH_2}$), 7.43-7.49 (m, 3H, Ar$\underline{H}$), 7.67-7.69 (m, 2H, Ar$\underline{H}$). ^{13}C NMR (125 MHz, $CDCl_3$, 25 °C): δ 21.2, 22.6, 55.1, 69.6, 74.7, 78.3, 121.0, 128.4, 130.1, 137.5, 162.9, 166.1, 167.6 and 168.6. Anal. calcd. for $C_{18}H_{18}N_2O_3$: C, 69.66; H, 5.85; N, 9.03; found: C, 69.71; H, 5.71, N, 9.08. HRMS calcd. for $C_{18}H_{18}N_2O_3$: *m/z* 310.1314; found: *m/z* 310.1314 (M^+).

4.6.1.4 Isopropyl 4-methyl-6-(4-nitrophenyl)-2-(prop-2-yn-1-yloxy)pyrimidine-5-carboxylate 29d

White solid. Yield: 94%. Rf: 0.5 (30% ethyl acetate/ hexane). Mp 96-98 °C. IR (KBr): ν_{max} 1520, 1554, 1606, 1721, 2937, 2985, 3084, 3109, 3279 cm^{-1}.^{1}H NMR (500 MHz, $CDCl_3$, 25 °C): δ 1.12 (d, *J* = 5.0 Hz, 6H, C-5 OCH($\underline{CH_3}$)$_2$), 2.50 (t, *J* = 2.5 Hz, 1H, CC$\underline{H}$), 2.62 (s, 3H, C-6 CH_3), 5.08-5.12 (m, 1H, C-5 O$\underline{CH}$(CH_3)$_2$ and 2 H C-2 O$\underline{CH_2}$), 7.83 (d, *J* = 5.0 Hz, 2H, Ar$\underline{H}$), 8.31 (d, *J* = 10.0 Hz, 2H, A$\underline{rH}$). ^{13}C NMR (125 MHz, $CDCl_3$, 25 °C): δ 21.3, 22.9, 55.4, 70.1, 75.0, 77.9, 121.1, 123.57, 129.5, 143.5, 148.7, 163.0, 163.9, 166.7 and 169.6. Anal. calcd. for $C_{18}H_{17}N_3O_5$: C, 60.84; H, 4.82; N, 11.83; found: C, 60.96; H, 4.61, N, 11.76. HRMS calcd. for $C_{18}H_{17}N_3O_5$: *m/z* 355.1168; found: *m/z* 355.1172 (M^+).

4.6.1.5 Isopropyl 4-methyl-6-(2-nitrophenyl)-2-(prop-2-yn-1-yloxy)pyrimidine-5-carboxylate 29e

White solid. Yield: 94%. Rf: 0.5 (30% ethyl acetate/ hexane). Mp 98-100 °C. IR (KBr): ν_{max} 1532, 1552, 1708, 2938, 3041, 3250 cm^{-1}.^{1}H NMR (500 MHz, $CDCl_3$, 25 °C): δ 0.94 (d, *J* = 5.0 Hz, 6H, C-5 OCH($\underline{CH_3}$)$_2$), 2.47 (t, *J* = 2.5 Hz, 1H, CC$\underline{H}$), 2.70 (s, 3H, C-6 CH_3), 4.91-4.96 (m, 1H, C-5 O$\underline{CH}$(CH_3)$_2$), 5.02 (d, *J* = 2.5 Hz, 2H, C-2 $\underline{OCH_2}$), 7.34 (d, *J* = 5.0 Hz, 1H, Ar$\underline{H}$), 7.61-7.70 (m, 2H, Ar$\underline{H}$), 8.20 (d, *J* = 10.0 Hz, 1H, Ar$\underline{H}$). ^{13}C NMR (125 MHz, $CDCl_3$, 25 °C): δ 21.3, 24.1, 55.7, 69.5, 75.2, 77.9, 119.9, 124.7, 130.0, 130.3, 133.4, 134.5, 147.5, 162.9, 165.4, 166.7 and 171.0. Anal. calcd. for $C_{18}H_{17}N_3O_5$: C, 60.84; H, 4.82; N, 11.83; found: C, 60.71; H, 4.67, N, 11.97. HRMS calcd. for $C_{18}H_{17}N_3O_5$: *m/z* 355.1168; found: *m/z* 355.1160 (M^+).

4.6.1.6 Ethyl 4,6-dimethyl-2-(prop-2-yn-1-yloxy)pyrimidine-5-carboxylate 29f

Colorless oil. Yield: 94%. Rf: 0.5 (30% ethyl acetate/hexane). IR (dichloromethane): ν_{max} 1510, 1577, 1715, 2989, 3257 cm^{-1}. ^1H NMR (500 MHz, $CDCl_3$, 25 °C): δ 1.40 (t, *J* = 7.5 Hz, 3H, C-5 $OCH_2\underline{CH_3}$), 2.48 (t, *J* = 2.5 Hz, 1H, C$\underline{CH}$), 2.52 (s, 3H, C-4 CH_3 and 3H, C-6 CH_3), 4.41 (q, *J* = 5.0 Hz, 2H, C-5 O$\underline{CH_2}CH_3$), 5.03 (d, *J* = 5.0 Hz, 2H, C-2 $\underline{OCH_2}$). ^{13}C NMR (125 MHz, $CDCl_3$, 25 °C): δ 14.1, 23.1, 52.6, 54.9, 74.6, 75.6, 120.9, 162.7, 167.3 and 168.2. Anal. calcd. for $C_{12}H_{14}N_2O_3$: C, 61.53; H, 6.02; N, 11.96; found: C, 61.64; H, 6.25, N, 11.78. HRMS calcd. for$C_{12}H_{14}N_2O_3$: *m/z* 234.1004; found: *m/z* 234.1006 (M^+).

4.6.2 Synthesis of triazole tethered pyrimidine-chloroquinoline hybrids

A solution of appropriate **29** (0.35 mmol) and **28/31** (0.35 mmol) in EtOH: H_2O (8:2, *v/v*) (10 mL), $CuSO_4.5H_2O$ (0.02 mmol) and sodium ascorbate (0.1 mmol) was stirred at ambient temperature. After completion (TLC), solvent was removed under vacuum. Water (30 mL) was then added to the residue and the product was extracted with DCM (2 x 20 mL). The organic phase was dried over anhydrous sodium sulphate. After removing DCM under reduced pressure, the crude product was purified by column chromatography using ethyl acetate/hexane mixtures as eluent to obtain pure **30a-l** and **32a-f**, respectively. The characteristic data of compounds prepared as above is given below.

4.6.2.1 Methyl 2-[(1-(3-(7-chloroquinolin-4-ylamino)propyl)-1*H*-1,2,3-triazol-4-yl)methoxy]-4-methyl-6-phenylpyrimidine-5-carboxylate 30a

White solid. Yield: 86%. Rf: 0.4 (10% ethyl acetate/MeOH). Mp 113-115 °C. IR (KBr): ν_{max} 1550, 1582, 1611, 1726, 2853, 2924, 3369 cm^{-1}.^1H NMR (500 MHz, $CDCl_3$, 25 °C): δ 2.29 (m, 2H, $NHCH_2\underline{CH_2}CH_2N$-), 2.56 (s, 3H, C-6 CH_3), 3.38 (m, 2H, $NH\underline{CH_2}CH_2CH_2N$-), 3.69 (s, 3H, C-5 O$\underline{CH_3}$), 4.49 (t, *J* = 7.5Hz, 2H, $NHCH_2CH_2\underline{CH_2}N$-), 5.62 (s, 2H, C-2 O$\underline{CH_2}$), 5.86 (br, 1H, NH, D_2O exchangeable), 6.34 (d, *J* = 5.0 Hz, 1H, CQ), 7.33-7.79 (m, 5H, Ar$\underline{H}$ and 3H, CQ), 7.92 (s, 1H, triazolyl H), 8.48 (s, 1H, CQ). ^{13}C NMR (125 MHz, $CDCl_3$, 25 °C): δ 22.8, 28.4, 39.9, 47.9, 52.5, 61.1, 98.8, 117.2, 120.1, 121.5, 123.6, 125.5, 128.1, 128.3, 128.5, 130.4, 135.0, 137.3, 143.8, 148.8, 149.6, 151.6, 163.4, 166.3, 168.6 and 169.0. HPLC [Methanol/H_2O, 25:75, 0.5 mL/min, 330 nm] t_R= 1.019 min. Anal. calcd. for $C_{28}H_{26}N_7ClO_3$: C, 61.82; H, 4.82; N, 18.02; found: C, 61.71; H, 4.80, N, 18.07. HRMS calcd. for $C_{28}H_{26}N_7ClO_3$: *m/z* 543.1786; found: *m/z* 544.1978 (M^++1).

4.6.2.2 Ethyl 2-[(1-(3-(7-chloroquinolin-4-ylamino)propyl)-1*H*-1,2,3-triazol-4-yl)methoxy]-4-methyl-6-phenylpyrimidine-5-carboxylate 30b

White solid. Yield: 84%. Rf: 0.4 (10% ethyl acetate/MeOH). Mp 93-95 °C. IR (KBr): ν_{max} 1552, 1583, 1719, 2956, 2982, 3326 cm^{-1}. ^1H NMR (500 MHz, $CDCl_3$, 25 °C): δ 1.04 (t, *J* = 7.5 Hz, 3H, C-5 $OCH_2\underline{CH_3}$), 2.32-2.34 (m, 2H, $NHCH_2\underline{CH_2}CH_2N$-), 2.57 (s, 3H, C-6 CH_3), 3.34 (m, 2H, $NH\underline{CH_2}CH_2CH_2N$-), 4.16 (q, *J* = 5.0 Hz, 2H, C-5 $O\underline{CH_2}CH_3$), 4.51 (t, *J* = 7.5 Hz, 2H, $NHCH_2CH_2\underline{CH_2}N$-) , 5.62 (s, 2H, C-2 $O\underline{CH_2}$), 6.12 (d, *J* = 5.0 Hz, 1H, CQ), 7.22 (d, *J* = 10.0 Hz, 1H, CQ), 7.41-7.47 (m, 3H, Ar<u>H</u>), 7.62 (d, *J* = 10.0 Hz, 2H, Ar<u>H</u>), 7.74 (s, 1H, CQ), 7.81 (s, 1H, triazolyl H), 7.96 (d, *J* = 10.0 Hz, 1H, CQ), 8.15 (d, *J* = 5.0 Hz, 1H, CQ). ^{13}C NMR (125 MHz, $CDCl_3$, 25 °C): δ 13.6, 22.7, 28.2, 40.3, 47.8, 61.0, 61.7, 97.7, 116.0, 120.4, 123.1, 123.6, 124.0, 126.2, 128.2, 128.4, 130.2, 137.1, 137.4, 142.9, 143.5, 146.2, 152.7, 163.4, 166.5, 168.0 and 168.9. HPLC [Methanol/H_2O, 25:75, 0.5 mL/min, 330 nm] t_R= 1.280 min. Anal. calcd. for $C_{29}H_{28}N_7ClO_3$: C, 62.42; H, 5.06; N, 17.57; found: C, 62.37; H, 4.80, N, 17.61. HRMS calcd. for $C_{29}H_{28}N_7ClO_3$: *m/z* 557.1942; found: *m/z* 558.2265 (M^++1).

4.6.2.3 Isopropyl 2-[(1-(3-(7-chloroquinolin-4-ylamino)propyl)-1*H*-1,2,3-triazol-4-yl)methoxy]-4-methyl-6-phenylpyrimidine-5-carboxylate 30c

White solid. Yield: 85%. Rf: 0.3 (10% ethyl acetate/MeOH). Mp 108-111 °C. IR (KBr): ν_{max} 1554, 1584, 1714, 2853, 2924, 2980, 3316 cm^{-1}.^1H NMR (500 MHz, $CDCl_3$, 25 °C): δ 1.07 (d, *J* = 5.0 Hz, 6H, C-5 $OCH(\underline{CH_3})_2$), 2.31 (m, 2H, $NHCH_2\underline{CH_2}CH_2N$-) 2.56 (s, 3H, C-6 CH_3), 3.34 (m, 2H, $NH\underline{CH_2}CH_2CH_2N$-), 4.50 (t, *J* = 7.5 Hz, 2H, $NHCH_2CH_2\underline{CH_2}N$-), 5.03-5.08 (m, 1H, C-5 $O\underline{CH}(CH_3)_2$), 5.60 (s, 2H, C-2 $O\underline{CH_2}$), 6.18 (d, *J* = 5.0 Hz, 1H, CQ), 7.24 (d, *J* = 5.0 Hz, 1H, CQ), 7.40-7.47 (m, 3H, Ar<u>H</u>), 7.62 (d, *J* = 10.0 Hz, 2H, Ar<u>H</u>), 7.77 (s, 1H, CQ), 7.80 (s, 1H, triazolyl H), 7.91 (d, *J* = 5.0 Hz, 1H, CQ), 8.25 (s, 1H, CQ). ^{13}C NMR (125 MHz, $CDCl_3$, 25 °C): δ 21.2, 22.6, 29.1, 40.2, 47.9, 61.0, 69.7, 98.1, 114.0, 116.5, 120.9, 123.9, 125.9, 128.3, 128.4, 130.2, 136.3, 137.4, 143.6, 145.0, 151.7, 163.3, 166.3, 167.5, 168.6 and 177.2. HPLC [Methanol/H_2O, 25:75, 0.5 mL/min, 330 nm] t_R= 1.390 min. Anal. calcd. for $C_{30}H_{30}N_7ClO_3$: C, 62.99; H, 5.29; N, 17.14; found: C, 62.71; H, 5.37, N, 17.33. HRMS calcd. for $C_{30}H_{30}N_7ClO_3$: *m/z* 571.2099; found: *m/z* 572.2127 (M^++1).

4.6.2.4 Isopropyl 2-[(1-(3-(7-chloroquinolin-4-ylamino)propyl)-1*H*-1,2,3-triazol-4-yl)methoxy]-4-methyl-6-(4-nitrophenyl)pyrimidine-5-carboxylate 30d

Pale yellow solid. Yield: 92%. Rf: 0.3 (10% ethyl acetate/MeOH). Mp 145-147 °C. IR (KBr): ν_{max} 1551, 1610, 1717, 2929, 2981, 3154, 3327 cm^{-1}.^{1}H NMR (500 MHz, $CDCl_3$, 25 °C): δ 1.11 (d, *J* = 10.0 Hz, 6H, C-5 OCH($\underline{CH_3}$)$_2$), 2.32-2.37 (m, 2H, NHCH$_2\underline{CH_2}$CH$_2$N-), 2.62 (s, 3H, C-6 CH_3), 3.42-3.46 (m, 2H, NH$\underline{CH_2}$CH$_2$CH$_2$N-), 4.55 (t, *J* = 7.5 Hz, 2H, NHCH$_2$CH$_2\underline{CH_2}$N-), 5.07-5.12 (m, 1H, C-5 O$\underline{CH}$(CH$_3$)$_2$), 5.40 (br, 1H, NH, D_2O exchangeable), 5.63 (s, 2H, C-2 O$\underline{CH_2}$), 6.38 (d, *J* = 5.0 Hz, 1H, CQ), 7.40 (d, *J* = 5.0 Hz, 1H , CQ), 7.67 (s, 1H, CQ), 7.69 (d, *J* = 5.0 Hz, 1H, CQ), 7.81 (d, *J* = 5.0 Hz, 2H, Ar$\underline{H}$), 7.96 (s, 1H, triazolyl H), 8.31 (d, *J* = 10.0 Hz, 2H, Ar$\underline{H}$), 8.54 (d, *J* = 5.0 Hz, 1H, CQ). ^{13}C NMR (125 MHz, $CDCl_3$, 25 °C): δ 21.3, 22.9, 28.4, 40.0, 47.9, 61.4, 70.1, 98.8, 117.1, 121.1, 123.5, 123.6, 125.6, 128.7, 128.7, 129.5, 135.1, 143.5, 143.7, 148.7, 151.8, 163.4, 164.2, 166.7 and 169.5. HPLC [Methanol/H_2O, 25:75, 0.5 mL/min, 330 nm] t_R= 1.381 min. Anal. calcd. for $C_{30}H_{29}N_8ClO_5$: C, 58.39; H, 4.74; N, 18.16; found: C, 58.46; H, 4.84, N, 18.31. HRMS calcd. for $C_{30}H_{29}N_8ClO_5$: *m/z* 616.1949; found: *m/z* 617.2198 (M^++1).

4.6.2.5 Isopropyl 2-[(1-(3-(7-chloroquinolin-4-ylamino)propyl)-1*H*-1,2,3-triazol-4-yl)methoxy]-4-methyl-6-(2-nitrophenyl)pyrimidine-5-carboxylate 30e

Pale yellow solid. Yield: 89%. Rf: 0.3 (10% ethyl acetate/MeOH). Mp 110-112 °C. IR (KBr): ν_{max} 1581, 1611, 1717, 2980, 3089, 3146, 3342 cm^{-1}.^{1}H NMR (500 MHz, $CDCl_3$, 25 °C): δ 0.94 (d, *J* = 5.0 Hz, 6H, C-5 OCH($\underline{CH_3}$)$_2$), 2.29-2.33 (m, 2H, NHCH$_2\underline{CH_2}$CH$_2$N-), 2.69 (s, 3H, C-6 CH_3), 3.38-3.40 (m, 2H, NH$\underline{CH_2}$CH$_2$CH$_2$N-), 4.50 (t, *J* = 5.0 Hz, 2H, NHCH$_2$CH$_2\underline{CH_2}$N-), 4.91-4.96 (m, 1H, C-5 O$\underline{CH}$(CH$_3$)$_2$), 5.57 (s, 2H, C-2 O$\underline{CH_2}$), 5.64 (br, 1H, NH, D_2O exchangeable), 6.37 (d, *J* = 5.0 Hz, 1H, CQ), 7.32-7.70 (m, 4H, Ar$\underline{H}$ and 1H, CQ), 7.74 (d, *J* = 10.0 Hz, 1H, CQ), 7.94 (s, 1H, triazolyl H), 8.16 (d, *J* = 10.0 Hz, 1H, CQ), 8.51 (d, *J* = 10.0 Hz, 1H, CQ). ^{13}C NMR (125 MHz, $CDCl_3$, 25 °C): 21.1, 23.9, 28.3, 39.8, 47.8, 61.3, 69.4, 98.9, 117.2, 119.6, 121.3, 123.5, 124.6, 125.5, 128.6, 129.9, 130.1, 133.4, 134.3, 135.0, 143.6, 147.1, 149.1, 149.4, 151.8, 163.1, 165.2, 166.3 and 171.0. HPLC [Methanol/H_2O, 25:75, 0.5 mL/min, 330 nm] t_R= 1.360 min. Anal. calcd. for $C_{30}H_{29}N_8ClO_5$: C, 58.39; H, 4.74; N, 18.16; found: C, 58.41; H, 4.80, N, 18.17. HRMS calcd. for $C_{30}H_{29}N_8ClO_5$: *m/z* 616.1949; found: *m/z* 617.2198 (M^++1).

4.6.2.6 Ethyl 2-[(1-(3-(7-chloroquinolin-4-ylamino)propyl)-1*H*-1,2,3-triazol-4-yl)methoxy]-4,6-dimethylpyrimidine-5-carboxylate 30f

White soild. Yield: 87%. Rf: 0.4 (10% ethyl acetate/MeOH). Mp 98-100 °C. IR (KBr): ν_{max} 1591, 1611, 1729, 2850, 2918, 2960, 3429 cm^{-1}.^{1}H NMR (500 MHz, $CDCl_3$, 25 °C): δ 1.40 (t, *J* = 5.0 Hz, 3H, C-5 $OCH_2\underline{CH_3}$), 2.28-2.33 (m, 2H, $NHCH_2\underline{CH_2}CH_2N$-), 2.50 (s, 3H, C-4 CH_3 and 3H, C-6 CH_3), 3.37-3.41 (m, 2H, $NH\underline{CH_2}CH_2CH_2N$-), 4.40 (q, *J* = 10.0 Hz, 2H, C-5 $O\underline{CH_2}CH_3$), 4.50 (t, *J* = 5.0 Hz, 2H, $NHCH_2CH_2\underline{CH_2}N$-) , 5.53 (s, 2H, C-2 $O\underline{CH_2}$), 5.83 (br, 1H, NH, D_2O exchangeable), 6.33 (d, *J* = 5.0 Hz, 1H, CQ), 7.31-7.33 (m, 1H, CQ), 7.70 (s, 1H, triazolyl H), 7.81 (d, *J* = 10.0, 1H, CQ), 7.91 (s, 1H, CQ), 8.47 (d, *J* = 5.0 Hz, 1H, CQ). ^{13}C NMR (125 MHz, $CDCl_3$, 25 °C): δ 14.1, 23.2, 28.4, 39.9, 47.9, 60.9, 61.6, 98.8, 117.3, 120.8, 121.7, 123.6, 125.4, 128.2, 135.0, 143.8, 148.8, 149.7, 151.6, 163.1, 167.3 and 168.3. HPLC [Methanol/H_2O, 25:75, 0.5 mL/min, 330 nm] t_R= 1.341 min. Anal. calcd. for $C_{24}H_{26}N_7ClO_3$: C, 58.12; H, 5.28; N, 19.77; found: C, 58.34; H, 5.33, N, 19.81. HRMS calcd. for $C_{24}H_{26}N_7ClO_3$: *m/z* 495.1786; found: *m/z* 496.1920 (M^++1).

4.6.2.7 Methyl 2-[(1-(2-(7-chloroquinolin-4-ylamino)ethyl)-1*H*-1,2,3-triazol-4-yl)methoxy]-4-methyl-6-phenylpyrimidine-5-carboxylate 30g

White solid. Yield: 89%. Rf: 0.4 (10% ethyl acetate/MeOH). Mp 163-165 °C. IR (KBr): ν_{max} 1551, 1579, 1610, 1724, 2950, 3075, 3290 cm^{-1}.^{1}H NMR (500 MHz, $CDCl_3$, 25 °C): δ 2.54 (s, 3H, C-6 CH_3), 3.68 (s, 3H, C-5 $\underline{OCH_3}$), 3.83-3.90 (m , 2H, $NH\underline{CH_2}CH_2N$-), 4.70 (t, *J* = 7.5 Hz, 2H, $NHCH_2\underline{CH_2}N$-), 5.63 (s, 2H, C-2 $O\underline{CH_2}$), 5.86 (br, 1H, NH, D_2O exchangeable), 6.41 (d, *J* = 5.0 Hz, 1H, CQ), 7.36 (d, *J* = 10.0 Hz, 1H, CQ), 7.41-7.48 (m, 3H, Ar$\underline{H}$), 7.60 (d, *J* = 10.0 Hz, 2H, Ar$\underline{H}$), 7.68 (d, *J* = 5.0 Hz, 2H, CQ), 7.95 (s, 1H, triazolyl H), 8.55 (s, 1H, CQ). ^{13}C NMR (125 MHz, $CDCl_3$, 25 °C): δ 22.8, 42.7, 48.5, 52.5, 60.9, 98.7, 120.0, 121.4, 124.4, 125.8, 128.1, 128.5, 130.4, 135.2, 137.3, 143.6, 149.0, 151.8, 163.4, 166.3, 168.5 and 169.0. HPLC [Methanol/H_2O, 25:75, 0.5 mL/min, 330 nm] t_R= 1.306 min. Anal. calcd. for $C_{27}H_{24}N_7ClO_3$: C, 61.19; H, 4.56; N, 18.50; found: C, 61.34; H, 4.67, N, 18.54. HRMS calcd. for $C_{27}H_{24}N_7ClO_3$: *m/z* 529.1629; found: *m/z* 530.1751 (M^++1).

4.6.2.8 Ethyl 2-[(1-(2-(7-chloroquinolin-4-ylamino)ethyl)-1*H*-1,2,3-triazol-4-yl)methoxy]-4-methyl-6-phenylpyrimidine-5-carboxylate 30h

White solid. Yield: 85%. Rf: 0.4 (10% ethyl acetate/MeOH). Mp 148-151 °C. IR (KBr): ν_{max} 1553, 1578, 1610, 1718, 2928, 2983, 3079, 3280 cm^{-1}.^{1}H NMR (500 MHz,

$CDCl_3$, 25 °C): δ 1.04 (t, *J* = 7.5 Hz, 3H, C-5 $OCH_2\underline{CH_3}$), 2.55 (s, 3H, C-6 CH_3), 3.86-3.88 (m, 2H, $NH\underline{CH_2}CH_2N$-), 4.16 (q, *J* = 5.0 Hz, 2H, C-5 $O\underline{CH_2}CH_3$), 4.71 (t, *J* =5Hz, 2H, $NHCH_2\underline{CH_2}N$-), 5.62 (s, 2H, C-2 $O\underline{CH_2}$), 6.14 (br, 1H, NH, D_2O exchangeable), 6.39 (d, *J* = 5.0 Hz, 1H, CQ), 7.35 (d, *J* = 10.0 Hz, 1H, CQ), 7.40-7.46 (m, 3H, Ar<u>H</u>), 7.59 (d, *J* = 5.0 Hz, 2H, Ar<u>H</u>), 7.72 (s, 1H, CQ), 7.74 (d, *J* = 10.0 Hz, 1H, CQ), 7.93 (s, 1H, triazolyl H), 8.50 (d, *J* = 5.0 Hz, 1H, CQ). ^{13}C NMR (125 MHz, $CDCl_3$, 25 °C): δ 13.6, 22.7, 42.8, 48.6, 60.9, 61.8, 98.7, 117.1, 120.4, 121.5, 124.3, 126.0, 128.0, 128.2, 128.4, 130.3, 135.5, 137.4, 143.8, 149.4, 151.2, 163.3, 166.5, 168.0 and 168.9. HPLC [Methanol/H_2O, 25:75, 0.5 mL/min, 330 nm] t_R= 1.275 min. Anal. calcd. for $C_{28}H_{26}N_7ClO_3$: C, 61.82; H, 4.82; N, 18.02; found: C, 61.68; H, 4.80, N, 18.16. HRMS calcd. for $C_{28}H_{26}N_7ClO_3$: *m/z* 543.1786; found: *m/z* 544.1853 (M^++1).

4.6.2.9 Isopropyl 2-[(1-(2-(7-chloroquinolin-4-ylamino)ethyl)-1*H*-1,2,3-triazol-4-yl)methoxy]-4-methyl-6-phenylpyrimidine-5-carboxylate 30i

White solid. Yield: 88%. Rf: 0.4 (10% ethyl acetate/MeOH). Mp 158-160 °C. IR (KBr): ν_{max} 1555, 1578, 1721, 2930, 2979, 3081, 3285 cm^{-1}.^{1}H NMR (500 MHz, $CDCl_3$, 25 °C): δ 1.07 (d, *J* = 5.0 Hz, 6H, C-5 $OCH(\underline{CH_3})_2$), 2.55 (s, 3H, C-6 CH_3), 3.85-3.87 (m, 2H, $NH\underline{CH_2}CH_2N$-), 4.71 (t, *J* = 5.0 Hz, 2H, $NHCH_2\underline{CH_2}N$-), 5.03-5.07 (m, 1H, C-5 $O\underline{CH}(CH_3)_2$), 5.62 (s, 2H, C-2 $O\underline{CH_2}$), 6.06 (br, 1H, NH, D_2O exchangeable), 6.41 (s, 1H, CQ), 7.36 (d, *J* = 5.0 Hz, 1H, CQ), 7.40-7.47 (m, 3H, Ar<u>H</u>), 7.60 (d, *J* = 5.0 Hz, 2H, CQ), 7.71-7.74 (m, 2H, Ar<u>H</u>), 7.94 (s, 1H, triazolyl H), 8.52 (s, 1H, CQ). ^{13}C NMR (125 MHz, $CDCl_3$, 25 °C): δ 21.3, 22.7, 42.8, 48.6, 61.0, 69.7, 120.9, 121.4, 124.3, 126.0, 128.3, 128.4, 130.2, 135.5, 137.4, 143.9, 163.3, 166.3, 167.5 and 168.6. HPLC [Methanol/H_2O, 25:75, 0.5 mL/min, 330 nm] t_R= 1.036 min. Anal. calcd. for $C_{29}H_{28}N_7ClO_3$: C, 62.42; H, 5.06; N, 17.57; found: C, 62.57; H, 5.15, N, 17.69. HRMS calcd. for $C_{29}H_{28}N_7ClO_3$: *m/z* 557.1942; found: *m/z* 558.2824 (M^++1).

4.6.2.10 Isopropyl 2-[(1-(2-(7-chloroquinolin-4-ylamino)ethyl)-1*H*-1,2,3-triazol-4-yl)methoxy]-4-methyl-6-(4-nitrophenyl)pyrimidine-5-carboxylate 30j

Pale yellow solid. Yield: 81%. Rf: 0.3 (10% ethyl acetate/MeOH). Mp 177-179 °C. IR (KBr): ν_{max} 1547, 1609, 1737, 2931, 2981, 3083, 3286 cm^{-1}.^{1}H NMR (500 MHz, $CDCl_3$, 25 °C): δ 1.11 (d, *J* = 5.0 Hz, 6H, C-5 $OCH(\underline{CH_3})_2$), 2.62 (s, 3H, C-6 CH_3), 3.88-3.91 (m, 2H, $NH\underline{CH_2}CH_2N$-), 4.73 (t, *J* = 5.0 Hz, 2H, $NHCH_2\underline{CH_2}N$-), 5.08-5.12

(m, 1H, C-5 O<u>CH</u>$(CH_3)_2$), 5.63 (s, 2H, C-2 O<u>CH_2</u>), 5.76 (br, 1H, NH, D_2O exchangeable), 6.41 (d, *J* = 5.0 Hz, 1H, CQ), 7.39 (d, *J* = 10.0 Hz, 1H , CQ), 7.67 (d, *J* = 10.0 Hz, 1H, CQ), 7.70 (s, 1H, CQ), 7.78 (d, *J* = 10.0 Hz, 2H, Ar<u>H</u>), 7.97 (s, 1H, triazolyl H), 8.29 (d, *J* = 10.0 Hz, 2H, Ar<u>H</u>), 8.55 (d, *J* = 5.0 Hz, 1H CQ). ^{13}C NMR (125 MHz, $CDCl_3$, 25 °C): 21.3, 22.9, 42.8, 48.6, 61.1, 70.1, 98.8, 117.2, 121.0, 121.2, 123.5, 124.3, 125.8, 128.7, 129.4, 135.2, 143.4, 143.5, 148.7, 148.9, 151.8, 163.3, 164.1, 166.6 and 169.5. HPLC [Methanol/H_2O, 25:75, 0.5 mL/min, 330 nm] t_R= 1.049 min. Anal.calcd. for $C_{29}H_{27}N_8ClO_5$: C, 57.76; H, 4.51; N, 18.58; found: C, 57.71; H, 4.76, N, 18.63. HRMS calcd. for $C_{29}H_{27}N_8ClO_5$: *m/z* 602.1793; found: *m/z* 603.1927 (M^++1).

4.6.2.11 Isopropyl 2-[(1-(2-(7-chloroquinolin-4-ylamino)ethyl)-1*H*-1,2,3-triazol-4-yl)methoxy]-4-methyl-6-(2-nitrophenyl)pyrimidine-5-carboxylate 30k

Pale yellow solid. Yield: 86%. Rf: 0.3 (10% ethyl acetate/MeOH). Mp 175-177 °C. IR (KBr): ν_{max} 1581, 1611, 1718, 2980, 3108, 3148, 3322 cm^{-1}.^{1}H NMR (500 MHz, $CDCl_3$, 25 °C): δ 0.94 (d, *J* = 5.0 Hz, 6H, C-5 OCH(<u>CH_3</u>)$_2$), 2.66 (s, 3H, C-6 CH_3), 3.86-3.90 (m, 2H, NH<u>CH_2</u>CH_2N-), 4.69 (t, *J* = 7.5 Hz, 2H, NHCH$_2$<u>CH_2</u>N-), 4.92-4.97 (m, 1H, C-5 O<u>CH</u>$(CH_3)_2$), 5.56 (s, 2H, C-2 O<u>CH_2</u>), 5.92 (br, 1H, NH, D_2O exchangeable), 6.42 (d, *J* = 5Hz, 1H, CQ), 7.29-7.68 (m, 3H, Ar<u>H</u> and 3H, CQ), 7.95 (s, 1H , triazolyl H), 8.13 (d, *J* = 10.0 Hz, 1H, Ar<u>H</u>), 8.54 (d, *J* = 5.0 Hz, 1H, CQ). ^{13}C NMR (125 MHz, $CDCl_3$, 25 °C): δ 21.1, 23.8, 42.7, 48.6, 61.2, 69.4, 98.8, 117.2, 119.7, 121.3, 124.0, 124.6, 125.8, 128.6, 129.9, 130.0, 133.3, 134.2, 135.2, 143.6, 147.2, 149.0, 151.8, 163.0, 165.2, 166.2 and 171.0. HPLC [Methanol/H_2O, 25:75, 0.5 mL/min, 330 nm] t_R= 1.066 min. Anal. calcd. for $C_{29}H_{27}N_8ClO_5$: C, 57.76; H, 4.51; N, 18.58; found: C, 57.81; H, 4.71, N, 18.43. HRMS calcd. for $C_{29}H_{27}N_8ClO_5$: *m/z* 602.1793; found: *m/z* 603.1927 (M^++1).

4.6.2.12 Ethyl 2-[(1-(2-(7-chloroquinolin-4-ylamino)ethyl)-1*H*-1,2,3-triazol-4-yl)methoxy]-4,6-dimethylpyrimidine-5-carboxylate 30l

White solid. Yield: 82%. Rf: 0.4 (10% ethyl acetate/MeOH). Mp 130-132 °C. IR (KBr): ν_{max} 1557, 1585, 1613, 1721, 2979, 3142, 3274 cm^{-1}. ^{1}H NMR (500 MHz, $CDCl_3$, 25 °C): δ 1.40 (t, *J* = 7.5 Hz, 3H, C-5 OCH$_2$<u>CH_3</u>), 2.49 (s, 3H, C-4 CH_3 and 3H, C-6 CH_3), 3.87-3.89 (m, 2H, NH<u>CH_2</u>CH_2N-), 4.41 (q, *J* = 10.0 Hz, 2H, C-5 O<u>CH_2</u>CH_3), 4.72 (t, *J* = 5.0 Hz, 2H, NHCH$_2$<u>CH_2</u>N-), 5.56 (s, 2H, C-2 O<u>CH_2</u>), 5.89 (br, 1H, NH, D_2O exchangeable), 6.41 (d, *J* = 5.0 Hz, 1H, CQ), 7.38 (d, *J* = 10.0 Hz, 1H,

CQ), 7.70 (d, *J* = 5.0 Hz, 2H, CQ), 7.96 (s, 1H, triazolyl H), 8.54 (d, *J* = 5.0 Hz, 1H, CQ). ^{13}C NMR (125 MHz, $CDCl_3$, 25 °C): δ 14.1, 23.2, 42.8, 48.6, 60.8, 61.6, 98.8, 117.2, 120.8, 121.3, 124.2, 125.9, 128.7, 135.2, 143.9, 148.9, 149.0, 151.8, 163.1, 167.3 and 168.3. HPLC [Methanol/H_2O, 25:75, 0.5 mL/min, 330 nm] t_R= 1.084 min. Anal. calcd. for $C_{23}H_{24}N_7ClO_3$: C, 57.32; H, 5.02; N, 20.34; found: C, 57.21; H, 4.89, N, 20.41. HRMS calcd. for $C_{23}H_{24}N_7ClO_3$: *m/z* 481.1629; found: *m/z* 482.1731 (M^++1).

4.6.2.13 Methyl 2-[(1-(7-chloroquinolin-4-yl)-1*H*-1,2,3-triazol-4-yl)methoxy]-4-methyl-6-phenylpyrimidine-5-carboxylate 32a

White soild. Yield: 82%. Rf: 0.3 (70% ethyl acetate/hexane). Mp 118-120 °C. IR (KBr): ν_{max} 1556, 1612, 1726, 2854, 2927, 2951, 3091, 3131 cm^{-1}.^{1}H NMR (500 MHz, $CDCl_3$, 25 °C): δ 2.61 (s, 3H, C-6 CH_3), 3.70 (s, 3H, C-5 $\underline{OCH_3}$), 5.83 (s, 2H, C-2 O$\underline{CH_2}$), 7.45- 7.50 (m, 3H, Ar$\underline{H}$ and 1H, CQ), 7.59 (d , *J* = 10.0 Hz, 1H, CQ), 7.68 (d, *J* = 10.0 Hz, 2H, Ar$\underline{H}$), 7.97 (d, *J* = 10.0 Hz, 1H, CQ), 8.17 (s, 1H, triazolyl H), 8.25 (d, *J* = 1.5 Hz, 1H, CQ), 9.06 (d, *J* = 5.0 Hz, 1H, CQ). ^{13}C NMR (125 MHz, $CDCl_3$, 25 °C): δ 22.8, 52.6, 61.0, 116.0, 120.3, 120.5, 124.5, 125.0, 128.2, 128.6, 129.0, 129.5, 130.5, 136.9, 137.3, 140.9, 144.4, 150.2, 151.4, 163.5, 166.4, 168.6 and 169.2. HPLC [Methanol/H_2O, 25:75, 0.5 mL/min, 330 nm] t_R= 1.054 min. Anal. calcd. for $C_{25}H_{19}N_6ClO_3$: C, 61.67; H, 3.93; N, 17.26; found: C, 61.54; H, 4.05, N, 17.45. HRMS calcd. for $C_{25}H_{19}N_6ClO_3$: *m/z* 486.1207; found: *m/z* 487.1464 (M^++1).

4.6.2.14 Ethyl 2-[(1-(7-chloroquinolin-4-yl)-1*H*-1,2,3-triazol-4-yl)methoxy]-4-methyl-6-phenylpyrimidine-5-carboxylate 32b

White solid. Yield: 88%. Rf: 0.3 (70% ethyl acetate/hexane). Mp 103-105 °C. IR (KBr): ν_{max} 1556, 1611, 1722, 2928, 2979, 3090, 3131 cm^{-1}.^{1}H NMR (500 MHz, $CDCl_3$, 25 °C): δ 1.06 (t, *J* = 7.5 Hz, 3H, C-5 OCH$_2\underline{CH_3}$), 2.62 (s, 3H, C-6 CH_3), 4.18 (q, *J* = 7.5 Hz, 2H, C-5 O$\underline{CH_2}$CH$_3$), 5.83 (s, 2H, C-2 O$\underline{CH_2}$), 7.44-7.49 (m, 3H, Ar$\underline{H}$ and 1H, CQ), 7.58-7.60 (m, 1H, CQ), 7.67 (d, *J* = 5.0 Hz, 2H, Ar$\underline{H}$), 7.97 (d, *J* = 10.0 Hz, 1H, CQ), 8.17 (s, 1H, triazolyl H), 8.25 (d, *J* = 1.5 Hz, 1H, CQ), 9.06 (d, *J* = 5.0 Hz, 1H, CQ). ^{13}C NMR (125 MHz, $CDCl_3$, 25 °C): δ 13.6, 22.8, 61.0, 61.8, 116.0, 120.5, 120.6, 124.5, 125.0, 128.2, 128.5, 129.0, 129.5, 130.3, 136.9, 137.4, 140.9, 144.4, 150.2, 151.3, 163.4, 166.6, 168.0 and 169.1. HPLC [Methanol/H_2O, 25:75, 0.5 mL/min, 330 nm] t_R= 1.408 min. Anal. calcd. for $C_{26}H_{21}N_6ClO_3$: C, 62.34; H, 4.23; N,

16.78; found: C, 62.31; H, 4.07, N, 16.89. HRMS calcd. for $C_{26}H_{21}N_6ClO_3$: *m/z* 500.1364; found: *m/z* 523.1345 (M^++23).

4.6.2.15 Isopropyl 2-[(1-(7-chloroquinolin-4-yl)-1*H*-1,2,3-triazol-4-yl)methoxy]-4-methyl-6-phenylpyrimidine-5-carboxylate 32c

White solid. Yield: 83%. Rf: 0.4 (70% ethyl acetate/hexane). Mp 123-125 °C. IR (KBr): ν_{max} 1558, 1592, 1611, 1719, 2936, 2979, 3089, 3130 cm^{-1}.^{1}H NMR (500 MHz, $CDCl_3$, 25 °C): δ 1.09 (d, *J* = 5.0 Hz, 6H, C-5 OCH($\underline{CH_3}$)$_2$), 2.61 (s, 3H, C-6 CH_3), 5.06-5.11 (m, 1H, C-5 O$\underline{CH}$(CH_3)$_2$), 5.82 (s, 2H, C-2 O$\underline{CH_2}$), 7.44-7.51 (m, 3H, Ar$\underline{H}$ and 1H, CQ), 7.59-7.61 (m, 1H, CQ), 7.67-7.69 (m, 2H, Ar$\underline{H}$), 7.98 (d, *J* = 10.0 Hz, 1H, CQ), 8.18 (s, 1H, triazolyl H), 8.25 (d, *J* = 5.0 Hz, 1H, CQ), 9.07 (d, *J* = 4.5 Hz, 1H, CQ). ^{13}C NMR (125 MHz, $CDCl_3$, 25 °C): δ 21.3, 22.7, 61.0, 69.7, 116.0, 120.5, 121.1, 124.5, 125.0, 128.3, 128.5, 129.0, 129.5, 130.3, 136.9, 137.4, 140.9, 144.5, 150.2, 151.4, 163.3, 166.4, 167.5 and 168.7. HPLC [Methanol/H_2O, 25:75, 0.5 mL/min, 330 nm] t_R= 1.402 min. Anal. calcd. for $C_{27}H_{23}N_6ClO_3$: C, 62.97; H, 4.50; N, 16.32; found: C, 62.71; H, 4.24, N, 16.47. HRMS calcd. for $C_{27}H_{23}N_6ClO_3$: *m/z* 514.1520; found: *m/z* 515.1683 (M^++1).

4.6.2.16 Isopropyl 2-[(1-(7-chloroquinolin-4-yl)-1*H*-1,2,3-triazol-4-yl)methoxy]-4-methyl-6-(4-nitrophenyl)pyrimidine-5-carboxylate32d

Pale yellow solid. Yield: 86%. Rf: 0.3 (70% ethyl acetate/hexane). Mp 97-100 °C. IR (KBr): ν_{max} 1584, 1610, 2853, 2925, 3088, 3126 cm^{-1}.^{1}H NMR (500 MHz, $CDCl_3$, 25 °C): δ 1.12 (d, *J* = 5.0 Hz, 6H, C-5 OCH($\underline{CH_3}$)$_2$), 2.65 (s, 3H, C-6 CH_3), 5.08-5.13 (m, 1H, C-5 O$\underline{CH}$(CH_3)$_2$), 5.82 (s, 2H, C-2 O$\underline{CH_2}$), 7.49 (d, *J* = 5.0 Hz, 1H , CQ), 7.61 (d, *J* = 10.0 Hz, 1H, CQ), 7.84 (d, *J* = 5.0 Hz, 2H, Ar$\underline{H}$), 7.98 (d, *J* = 10.0 Hz, 1H, CQ), 8.18 (s, 1H, triazolyl H), 8.26 (d, *J* = 2.0 Hz, 1H, CQ), 8.32 (d, *J* = 10.0 Hz, 2H, Ar$\underline{H}$), 9.07 (d, *J* = 5.0 Hz, 1H, CQ). ^{13}C NMR (125 MHz, $CDCl_3$, 25 °C): 21.3, 23.0, 61.2, 70.2, 116.0, 120.5, 121.3, 123.6, 124.4, 125.0, 129.0, 129.5, 137.0, 143.4, 144.1, 148.7, 150.2, 151.4, 163.4, 164.2, 166.6 and 169.6. HPLC [Methanol/H_2O, 25:75, 0.5 mL/min, 330 nm] t_R= 1.381 min. Anal. calcd. for $C_{27}H_{22}N_7ClO_5$: C, 57.91; H, 3.96; N, 17.51; found: C, 57.83; H, 3.80, N, 17.55. HRMS calcd. for $C_{27}H_{22}N_7ClO_5$: *m/z* 559.1371; found: *m/z* 582.1384 (M^++23).

4.6.2.17 Isopropyl 2-[(1-(7-chloroquinolin-4-yl)-1*H*-1,2,3-triazol-4-yl)methoxy]-4-methyl-6-(2-nitrophenyl)pyrimidine-5-carboxylate 32e

White solid. Yield: 87%. Rf: 0.3 (70% ethyl acetate/hexane). Mp 168-170 °C. IR (KBr): ν_{max} 1555, 1613, 1717, 2982, 3092, 3155 cm^{-1}.^{1}H NMR (500 MHz, $CDCl_3$, 25 °C): δ 0.95 (d, *J* = 10.0 Hz, 6H, C-5 OCH($\underline{CH_3}$)$_2$), 2.72 (s, 3H, C-6 CH_3), 4.92-4.97 (m, 1H, C-5 O$\underline{CH}$(CH_3)$_2$), 5.75 (s, 2H, C-2 O$\underline{CH_2}$), 7.35-7.37 (m, 1H, CQ), 7.52 (d, *J* = 2.5 Hz, 1H, CQ), 7.59-7.70 (m, 3H, Ar$\underline{H}$), 7.99 (d, *J* = 5.0 Hz, 1H, CQ), 8.12 (s, 1H, triazolyl H), 8.19 (d, *J* = 10.0 Hz, 1H, CQ), 8.24 (d, *J* = 5.0 Hz, 1H, Ar$\underline{H}$), 9.06 (d, *J* = 5.0 Hz, 1H, CQ). ^{13}C NMR (125 MHz, $CDCl_3$, 25 °C): δ 21.0, 23.8, 61.1, 69.3, 116.0, 119.7, 120.5, 124.5, 124.5, 124.9, 128.8, 129.3, 129.8, 129.9, 133.2, 134.1, 136.8, 140.8, 144.0, 147.2, 150.1, 151.3, 163.0, 165.1, 166.4 and 171.0. HPLC [Methanol/H_2O, 25:75, 0.5 mL/min, 330 nm] t_R= 1.413 min. Anal. calcd. for $C_{27}H_{22}N_7ClO_5$: C, 57.91; H, 3.96; N, 17.51; found: C, 57.84; H, 3.94, N, 17.27. HRMS calcd. for $C_{27}H_{22}N_7ClO_5$: *m/z* 559.1371; found: *m/z* 582.1384 (M^++23).

4.6.2.18 Ethyl 2-[(1-(7-chloroquinolin-4-yl)-1*H*-1,2,3-triazol-4-yl)methoxy]-4,6-dimethylpyrimidine-5-carboxylate 32f

White solid. Yield: 85%. Rf: 0.3 (70% ethyl acetate/hexane). Mp 112-114 °C. IR (KBr): ν_{max} 1558, 1611, 1723, 2853, 2924, 3073 cm^{-1}.^{1}H NMR (500 MHz, $CDCl_3$, 25 °C): δ 1.41 (t, *J* = 5.0 Hz, 3H, C-5 OCH$_2\underline{CH_3}$), 2.55 (s, 3H, C-4 CH_3 and 3H, C-6 CH_3), 4.42 (q, *J* = 5.0 Hz, 2H, C-5 O$\underline{CH_2}$CH$_3$), 5.75 (s, 2H, C-2 O$\underline{CH_2}$), 7.50 (d, *J* = 4.5 Hz, 1H, CQ), 7.61 (d , *J* = 10.0 Hz, 1H, CQ), 7.98 (d, *J* = 10.0 Hz, 1H, CQ), 8.17 (s, 1H, triazolyl H), 8.26 (d, *J* = 1.5 Hz, 1H, CQ), 9.07 (d, *J* = 5.0 Hz, 1H, CQ). ^{13}C NMR (125 MHz, $CDCl_3$, 25 °C): δ 14.2, 23.3, 60.9, 61.7, 116.0, 120.6, 121.0, 124.5, 124.9, 129.0, 129.5, 137.0, 140.9, 144.5, 150.2, 151.4, 163.1, 167.3 and 168.4. HPLC [Methanol/H_2O, 25:75, 0.5 mL/min, 330 nm] t_R= 1.341 min. Anal. calcd. for $C_{21}H_{19}N_6ClO_3$: C, 57.47; H, 4.36; N, 19.15; found: C, 57.24; H, 4..13, N, 19.31. HRMS calcd. for $C_{21}H_{19}N_6ClO_3$: *m/z* 438.1207; found: *m/z* 438.1212 (M^+).

4.7 *In vitro* antiplasmodial assay

All samples were tested in triplicate against CQ^S strain of *P. falciparum* (NF54). Hybrids **30a-f** and **32h-l**, which were most active against CQ^S strain of *P. falciparum* (NF54) were also tested against CQ^R strain of *P. falciparum* (Dd2). Continuous *in vitro* cultures of asexual erythrocyte stages of *P. falciparum* were maintained using a modified method of Trager and Jensen [76]. Quantitative assessment of *in vitro*

antiplasmodial activity was determined *via* the parasite lactate dehydrogenase assay using a modified method described by Makler [77].

Stock solutions (20 mg/mL)of the test samples were prepared in 100% DMSO and stored at -20ºC. Samples which were not completely soluble were tested as a suspension. Further dilutions were prepared on the day of the experiment. CQ and ASN were used as the reference drugs in all experiments. A full dose-response was performed for all compounds to determine the concentration inhibiting 50% of parasite growth (IC_{50} value). Test samples were tested at a starting concentration of 100 µg/mL, which was then serially diluted 2-fold in complete medium to give 10 concentrations; with the lowest concentration being 0.2 µg/mL. The same dilution technique was used for all samples. Active compounds were retested at a starting concentration of 10 µg/mL or 1000 ng/mL. Reference drugs were tested at a starting concentration of 1000 ng/mL. The highest concentration of solvent to which the parasites were exposed to had no measurable effect on the parasite viability (data not shown). The IC_{50} values were obtained using a non-linear dose-response curve fitting analysis via Graph Pad Prism v.4.0 software.

4.8 Cytotoxicity assay

Hybrids **30a-f** and **32h-l**, which were active against CQ^S strain (NF54) and CQ^R strain of *P. falciparum* (Dd2) were also screened for *in vitro* cytotoxicity against mammalian Vero cell line using 3-(4,5-dimethylthiazol-2-yl)-2,5-diphenyltetrazoliumbromide (MTT)-assay performed in triplicate. MTT-assay is used as colorimetric assay for cellular growth and survival, and compares well with other available assays [78,79]. The tetrazolium salt MTT was used to measure all growth and chemosensitivity. The test compounds were stored at -20 °C until use. Dilutions were prepared on the day of the experiment. Emetine was used as the reference drug in all experiments. The initial concentration of emetine was 100 µg/mL, which was serially diluted in complete medium with 10-fold dilutions to give 6 concentrations, the lowest being 0.001 µg/mL. The same dilution technique was applied to all test samples. The highest concentration of solvent to which the cells were exposed to had no measurable effect on the cell viability (data not shown). The 50% inhibitory concentration IC_{50} values were obtained from full dose-response curves, using a non-linear dose-response curve fitting analysis *via* Graph Pad Prism v.4 software.

5. Acknowledgements

KS and RC are thankful to CSIR, New Delhi (Project No. 01(2687)12 EMR-II) for financial assistance and for SRF to RC and GNDU for research facilities. The University of Cape Town, South African Medical Research Council, and South African Research Chairs Initiative of the Department of Science and Technology, administered through the South African National Research Foundation are gratefully acknowledged for support (K.C). We thank Prof. Peter J. Smith and Dr. Carmen de Kock of the University of Cape Town, Department of Medicine for antiplasmodial assays.

6. References

[1] WHO World malaria report, 2017. World Health Organization, Geneva, Switzerland, 2017.

[2] K.B. Seydel, S.D. Kampondeni, C. Valim, M.J. Potchem, D.A. Milner, F.W. Muwalo, G.L. Birbeck, W.G Bradley, L.L. Fox, S.J. Glover, C.A. Hammond, R.S Heyderman, C.A Chilingulo, M.E. Molyneux, T.E. Taylor, Brain swelling and death in children with cerebral malaria, N. Engl. J. Med. 372 (2015) 1126-1137.

[3] S.J. Rogerson, L. Hviid, P.E. Duffy, R.F.G. Leke, D.W. Taylor, Malaria in pregnancy: pathogenesis and immunity, Lancet Infect. Dis. 7 (2007) 105-117.

[4] B.P Goncalves, C.-Y. Huang, R. Morrison, S. Holte, E. Kabyemela, R. Prevots, M. Fried, P.E. Duffy, Parasite burden and severity of malaria in Tanzanian children, N. Engl. J. Med. 370 (2014) 1799-1808.

[5] L.S. Garcia, Malaria, Clin. Lab. Med. 30 (2010) 93-129.

[6] T. Bousema, C. Drakeley, Epidemiology and infectivity of *Plasmodium falciparum* and *Plasmodium vivax* gametocytes in relation to malaria control and elimination Clin. Microbiol. Rev. 24 (2011) 377-410.

[7] R.E Howes, R.C. Reiner JR., K.E. Battle J., Longbottom, B. Mappin, D. Ordanovich, A.J Tatem, C. Drakeley, P.W. Gething, P.A. Zimmerman, D.L. Smith, S.I. Hay, *Plasmodium vivax* transmission in Africa, PLoS Negl. Trop. Dis. 9 (2015) 1-27.

[8] S.A. Mikolajczak, A.M. Vaughan, N. Kangwanrangsan, W. Roobsoong, M. Fishbaugher, N. Yimamnuaychok, N. Rezakhani, V. Lakshmanan, N. Singh, A.

Kaushansky, N. Camargo, M. Baldwin, S.E. Lindner, J.H Adams, J. Sattabongkot, S.H.I Kappe, *Plasmodium vivax* liver stage development and hypnozoite persistence in human liver-chimeric mice, Cell Host Microbe 17 (2015) 526-535.

[9] L. Dembele, J.-F. Franetich, A. Lorthiois, A. Gego, A.-M. Zeeman, C.H.M. Kocken, R. Le Grand, N. Dereuddre-Bosquet, G.-J. van Gemert, R. Sauerwein, J.-C. Vaillant, L. Hannoun, M.J. Fuchter, T.T. Diagana, N.A. Malmquist, A. Scherf, G. Snounou, D. Mazier, Persistence and activation of malaria hypnozoites in long-term primary hepatocyte cultures, Nat. Med. 20 (2014) 307-312.

[10] W.E. Collins, G.M. Jeffery, *Plasmodium malariae*: Parasite and Disease, Clin. Microbiol. Rev. 20 (2007) 579-592.

[11] M. Muller, P. Schlagenhauf, *Plasmodium knowlesi* in travellers, update 2014, Int J Infect Dis 22 (2014) 55-64.

[12] T-H. T. Tang, A. Salas, M. Ali-Tammam, M.D.C. Martinez, M. Lanza, E. Arroyo, J.M. Rubio, First case of detection of *Plasmodium knowlesi* in Spain by real time PCR in a traveller from Southeast Asia, Malaria J. 9 (2010) 219-225.

[13] S. Antinori, L. Galimberti, L. Milazzo, M. Corbellino, *Plasmodium knowlesi*: The emerging zoonotic malaria parasite, Acta Tropica 125 (2013) 191-201.

[14] D.E. Neafsey, R.M. Waterhouse, M.R. Abai et al. Highly evolvable malaria vectors: The genomes of 16 Anopheles mosquitoes, Science 347 (2015) 6217 1258522.

[15] P.M. O‟Neill, V.E. Barton, S.A. Ward, The molecular mechanism of action of artemisinin- The debate continues, Molecules 15 (2010) 1705-1721.

[16] N.M. Douglas, N.M. Anstey, B.J. Angus, F. Nosten, R.N. Price, Artemisinin combination therapy for *vivax* malaria, Lancet Infect. Dis. 10 (2010) 405-416.

[17] M. Giobbia, E. Tonon, A. Zanatta, L. Cesaris, A. Vaglia, Late recrudescence of *Plasmodium falciparum* malaria in a pregnant woman: a case report Int. J. Infect. Dis. 9 (2005) 234-235.

[18] W. Ittarat, A.L. Pickard, P. Rattanasinganchan, P. Wilairatana, S. Looareesuwan, K. Emery, J. Low, R. Udomsangpetch, S.R. Meshnick, Recrudescence in artisunate-treated patients with *falciparum* malaria is dependent on parasite burden not on parasite factors, Am. J. Trop. Med. Hyg. 68 (2003) 147-152.

[19] J.K. Baird, S.L. Hoffman, Primaquine therapy for malaria,. Clin. Infect. Dis. 39 (2004) 1336-1345.

[20] E.A. Ashley, J. Recht, N.J. White, Primaquine: the risks and the benefits, Malaria J. 13 (2014) 418-425.

[21] K.L. Burgoine, G. Bancone, F. Nosten, The reality of using primaquine, Malaria J. 9 (2010) 376-381.

[22] T.E. Wellems, C.V. Plowe, Chloroquine-resistant malaria, J. Infect. Dis. 184 (2001) 770-776.

[23] F. Koukouikila-Koussounda, D. Bakoua, A. Fesser, M. Nkombo, C. Vouvoungui, F. Ntoumi, High prevalence of sulphadoxine–pyrimethamine resistance-associated mutations in *Plasmodium falciparum* field isolates from pregnant women in Brazzaville, Republic of Congo, Infect. Gen. Evol. 33 (2015) 32-36.

[24] L. Paloque, A.P. Ramadani, O. Mercereau-Puijalon, J.-M. Augereau, F. Benoit-Vical, *Plasmodium falciparum*: multifaceted resistance to artemisinins, Malaria J. 15 (2016) 149-161.

[25] E.A. Ashley, M. Dhorda, R.M. Fairhurst et al. Spread of Artemisinin resistance in *Plasmodium falciparum* malaria, N. Engl. J. Med. 371 (2014) 411-423.

[26] S.L. Hargreaves, B.L. Pilkington, S.E. Russell, P.A. Worthington, The synthesis of substituted pyridylpyrimidine fungicides using palladium-catalysed cross-coupling reactions, Tetrahedron Lett. 41 (2000) 1653-1656.

[27] K.S. Jain, T.S. Chitre, P.B. Miniyar, M.K. Kathiravan, V.S. Bendre, V.S. Veer, S.R. Shahane, C.J. Shishoo, Biological and medicinal significance of pyrimidines, Curr. Sci. 90 (2006) 793-803.

[28] C.M. Galmarini, J.R. Mackey, C. Dumontet, Nucleoside analogues and nucleobases in cancer treatment, Lancet Oncol. 3 (2002) 415−424.

[29] S.J. Foote, D. Galatis, A.F. Cowman, Amino acids in the dihydrofolate reductase-thymidylate synthase gene of *Plasmodium falciparum* involved in cycloguanil resistance differ from those involved in pyrimethamine resistance, Proc. Natl. Acad. Sci. U.S.A. 87 (1990) 3014-3017.

[30] D.S. Barnett, R.K. Guy, Antimalarials in development in 2014, Chem. Rev. 114 (2014) 11221-11241.

[31] J.J. Walsh, A. Bell, Hybrid drugs for malaria, Curr. Pharm. Des. 15 (2009) 2970-2985.

[32] S. Vandekerckhov, M. Dhooghe, Quinoline-based antimalarial hybrid compounds, Bioorg. Med. Chem. 23 (2015) 5098-5119.

[33] R. Oliveira, D. Miranda, J. Magalhaes, R. Capela, M.J. Perry, P.M. O'Neill, R. Moreira, F. Lopes, From hybrid compounds to targeted drug delivery in antimalarial therapy, Bioorg. Med. Chem. 23 (2015) 5120-5130.

[34] A. Kumar, D. Paliwal, D. Saini, A. Thakur, S. Aggarwal, D. Kaushik, A comprehensive review on synthetic approach for antimalarial agents, Eur. J. Med. Chem. 85 (2014) 147-178.

[35] M.A. Biamonte, J. Wanner, K.G. Le Roch, Recent advances in malaria drug discovery, Bioorg. Med. Chem. Lett. 23 (2013) 2829-2843.

[36] M. Njoroge, N.M. Njuguna, P. Mutai, D.S.B. Ongarora, P.W. Smith, K. Chibale, Recent approaches to chemical discovery and development against malaria and the neglected tropical diseases human African trypanosomiasis and schistosomiasis, Chem. Rev. 114 (2014) 11138-11163.

[37] K. Singh, T. Kaur, Pyrimidine-based antimalarials: design strategies and antiplasmodial effects, Med. Chem. Commun. 7 (2016) 749-768.

[38] S. Manohar, V.S. Pavan, D. Taylor, D. Kumar, P. Ponnan, L. Wiesner, D.S. Rawat, Highly active 4-aminoquinoline–pyrimidine based molecular hybrids as potential next generation antimalarial agents, RSC Adv. 5 (2015) 28171-28186 and references cited therein.

[39] D. Kumar, S.I. Khan, B.L. Tekwani, P. Ponnan, D.S. Rawat, 4-Aminoquinoline-pyrimidine hybrids: Synthesis, antimalarial activity, heme binding and docking studies, Eur. J. Med. Chem. 89 (2015) 490-502.

[40] M. Sharma, V. Chaturvedi, Y.K. Manju, S. Bhatnagar, K. Srivastava, S.K. Puri, P.M.S. Chauhan, Substituted quinolinyl chalcones and quinolinyl pyrimidines as a new class of anti-infective agents, Eur. J. Med. Chem. 44 (2009) 2081-2091.

[41] S. Manohar, U.C. Rajesh, S.I. Khan, B.L. Tekwani, D.S. Rawat. Novel 4-aminoquinoline-pyrimidine based hybrids with improved in vitro and *in vivo* antimalarial activity, ACS Med. Chem. Lett. 3 (2012) 555-559.

[42] S. I. Pretorius, W. J. Breytenbach, C. D. Kock, P. J. Smith, D. D. N'Da, Synthesis, characterization and antimalarial activity of quinoline–pyrimidine hybrids, Bioorg. Med. Chem. 21 (2013) 269–277.

[43] H. Kaur, M. Machado, C. de Kock, P. Smith, K. Chibale, M. Prudencio, K. Singh, Primaquine-pyrimidine hybrids: Synthesis and dual-stage antiplasmodial activity, Eur. J. Med. Chem. 101 (2015) 266-273.

[44] K. Singh, H. Kaur, P. Smith, C. D. Kock, K. Chibale, and J. Balzarini, Quinoline–pyrimidine hybrids: Synthesis, antiplasmodial activity, SAR, and mode of action studies, J. Med. Chem. 57 (2014) 435-448.

[45] H. Kaur, J. Balzarini, C. de Kock, P.J. Smith, K. Chibale, K. Singh, Synthesis, antiplasmodial activity and mechanistic studies of pyrimidine-5-carbonitrile and quinoline hybrids, Eur. J. Med. Chem. 101 (2015) 52-62.

[46] J. Hou, X. Liu, J. Shen J, G. Zhao, P.G. Wang, The impact of click chemistry in medicinal chemistry, Expert Opin. Drug Discov. 7 (2012) 489-501.

[47] A. Lauria, R. Delisi, F. Mingoia, A. Terenzi, A. Martorana, G. Barone, A.M. Almerico, 1,2,3-Triazole in heterocyclic compounds endowed with biological activity, through 1,3-dipolar cycloadditions, Eur. J. Org. Chem. 16 (2014) 3289-3306.

[48] A. Ayati, S. Emami, A. Foroumadi, The importance of triazole scaffold in the development of anticonvulsant agents, Eur. J. Med. Chem. 109 (2016) 380-392.

[49] P. Bignelli, Aldureids of ethylic acetoacetate and ethylic oxaloacetate, Gazz. Chim. Ital. 23 (1893) 360–416.

[50] K. Singh, K. Singh, An efficacious protocol for the oxidation of 3,4-dihydropyrimidin-2(1*H*)-ones using pyridinium chlorochromate as catalyst, Aust. J. Chem. 61 (2008) 910–913.

[51] K. Singh, K. Singh, B. Wan, S. Franzblau, K. Chibale, J. Balzarini, Facile transformation of Biginelli pyrimidin-2(1*H*)-ones to pyrimidines. *In vitro* evaluation as inhibitors of *Mycobacterium tuberculosis* and modulators of cytostatic activity, Eur J. Med. Chem. 46 (2011) 2290–2294.

[52] J.L. Vennerstrom, W.Y. Ellis, A.L. Ager, S.L. Anderaen Jr, L. Gerena, W.K. Milhoust, Bisquinolines. 1. N,N-Bis(7-chloroquinolin-4-yl)alkanediamines with potential against chloroquine-resistant malaria, J. Med. Chem. 35 (1992) 2129-2134.

[53] K. Singh, H. Kaur, K. Chibale, J. Balzarini, S. Little, P.V Bharatam, 2-Aminopyrimidine based 4-aminoquinoline anti-plasmodial agents. Synthesis, biological activity, structure–activity relationship and mode of action studies, Eur. J. Med. Chem. 52 (2012) 82–97.

[54] C.A. Lipinski, F. Lombardo, B.W. Dominy, P.J. Feeney, Experimental and computational approaches to estimate solubility and permeability in drug discovery and development settings, Adv. Drug Delivery Rev. 46 (2001) 3−26.

[55] A. Avdeef, Physicochemical profiling (solubility, permeability and charge state), Curr. Top. Med. Chem. 1 (2001) 277−351.

[56] T.J. Egan, R. Hunter, C.H. Kaschula, H.M. Marques, A. Misplon, J. Walden, Structure-function relationships in aminoquinolines: Effect of amino and chloro groups on quinoline-hematin complex formation, inhibition of β-Hematin formation, and antiplasmodial activity, J. Med. Chem. 43 (2000) 283-291.

[57] D.C. Warhurst, J.C. Craig, I.S. Adagu, D.J. Meyer, S.Y. Lee, The relationship of physico-chemical properties and structure to the differential antiplasmodial activity of the cinchona alkaloids, Malaria. J. 2 (2003) 26.

[58] M. Steyn D.D. N'Da, J.C. Breytenbach, P.J. Smith, S. Meredith, W.J. Breytenbach, Synthesis and antimalarial activity of ethylene glycol oligomeric ethers of artemisinin, J. Pharm. Pharmacol.63 (2011) 278−286.

[59] T. Ossowski, M.O.F. Goulart, F.C. de Abreu, A.E.G. Sant'Ana, P.R.B. Miranda, C.O. Costa, A. Liwo, P. Falkowski, D. Zarzeczanska, Determination of the p*Ka* values of some biologically active and inactive hydroxyquinones, J. Braz. Chem. Soc. 19 (2008) 175-183.

[60] M. Foley, L. Tilley, Quinoline antimalarials: Mechanism of actions and resistance, Int. J. Parasitol. 27 (1997) 231-240.

[61] A. Dorn, R. Stoffel, H. Matile, A. Bubendorf, R.G. Ridley, Malarial haemozoin/β-haematin supports haem polymerization in the absence of protein, Nature 374 (1995) 269-271.

[62] T.J. Egan, W.W. Mavuso, D. Ross, H.M. Marques, Thermodynamic factors controlling the interaction of quinoline antimalarial drugs with ferritoporphyrin IX J. Inorg. Biochem. 68 (1997) 137-145.

[63] J.K. Natarajan, J.N. Alumasa, K. Yearick, K.A. Ekoue-Kovi, L.B. Casabianca, A.C. de Dios, C. Wolf, P.D. Roepe, 4-N-, 4-S-, and 4-O-Chloroquine analogues: Influence of side chain length and quinolyl nitrogen p*Ka* on activity vs chloroquine resistant malaria, J. Med. Chem. 51 (2008) 3466-3479.

[64] T.J. Egan, Interactions of quinoline antimalarials with hematin in solution, J. Inorg. Biochem. 100 (2006) 916-926.

[65] P. Gans, A. Sabatini, A. Vacca, Investigation of equilibria in solution. Determination of equilibrium constants with the HYPERQUAD suite of programs, Talanta 43 (1996) 1739-1753.

[66] T.J. Egan, D.C. Ross, P.A. Adams, Quinoline anti-malarial drugs inhibit spontaneous formation of β-haematin (malaria pigment), FEBS Lett. 352 (1994) 54-57.

[67] N. Basilico, D. Monti D, Olliaro, D. Taramelli, Non-iron porphyrins inhibit β-haematin (malaria pigment) polymerisation, FEBS Lett. 409 (1997) 297-299.

[68] M.J. Dascombe, M.G.B. Drew, H. Morris, P. Wilairat, S. Auparakkitanon, W.A. Moule, S. Alizadeh-Shekalgourabi, P.G. Evans, M. Lloyd, A.M. Dyas, P. Carr, F.M.D Ismail, Mapping antimalarial pharmacophores as a useful tool for the rapid discovery of drugs effective in vivo: Design, construction, characterization, and pharmacology of metaquine, J. Med. Chem. 48 (2005) 48:5423-5436.

[69] S.R. Meshnick, Quinoline as intercalator hypothesis revived, Parasitol Today 6 (1990) 77-79.

[70] W.D. Wilson, R.L. Jones, Intercalating drugs: DNA binding and molecular pharmacology, Adv. Pharmacol. Chemoether. 18 (1981) 177-222.

[71] J. Cheng, R. Zeidan, S. Mishra, A. Liu, S.H. Pun, R.P. Kulkarni, G.S. Jensen, N.C. Bellocq, M.E. Davis, Structure-function correlation of chloroquine and analogues as transgene expression enhancers in nonviral gene delivery, J. Med. Chem. 49 (2006) 6522-6531.

[72] Y. Pollack, A.L. Katzen, D.T. Spira, J. Golenser, The genome of Plasmodium falciparum. I: DNA base composition, Nucleic Acids Res. 10 (1982) 539-546.

[73] H.A. Benesi, J.H. Hildebrand, A Spectrophotometric investigation of the interaction of iodine with aromatic hydrocarbons, J. Am. Chem. Soc. 71 (1949) 2703-2707.

[74] Mudasir, E.T. Wahyuni, D.H. Tjahjono, N. Yoshioka, H. Inoue, Spectroscopic studies on the thermodynamic and thermal denaturation of the CT-DNA binding of methylene blue, Spectrochim. Acta Part A 77 (2010) 528-534.

[75] J.L. Allison, R.L. O'Brien, F.E. Hahn, DNA reaction with chloroquine, Science 149 (1965) 1111–1113.

[76] W. Trager, J. B. Jensen, Human malaria parasite in continuous culture, Science 193 (1976) 673- 675.

[77] M. T. Makler, J. M. Ries, J. A. Williams, J. E. Bancroft, R. C. Piper, B. L. Gibbins, D. J. Hinrichs, Parasite lactate dehydrogenase as an assay for *Plasmodium falciparum* drug sensitivity, Am J Trop Med Hyg, 48 (1993) 739-741.

[78] L.V. Rubinstein, R.H. Shoemaker, K.D. Paull, R.M. Simon, S. Tosini, P. Skehan, D.A. Scudiero, A. Monks, M.R. Boyd, Comparison of in vitro anticancer-drug-screening data generated with a tetrazolium assay versus a protein assay against a diverse panel of human tumor cell lines, J Natl Cancer Inst 82 (1990) 1113-1118.

[79] T. Mosmann, Rapid colorimeteric assay for cellular growth and survival: Application to proliferation and cytotoxicity assay, J Immunol methods 65 (1983) 55-63.

- New antimalarial compounds
- Efficacious synthesis
- Binding with DNA
- Binding with Heme and μ-oxoheme